Multi-energy microgrids

An optimal despatch model for water-energy nexus

Jalilian, Faezeh ; Mirzaei, Mohammad Amin ; Zare, Kazem; Mohammadiivatloo, Behnam; Marzband, Mousa; Anvari-Moghaddam, Amjad

Published in:
Sustainable Cities and Society

DOI (link to publication from Publisher):
10.1016/j.scs.2021.103573

Publication date:
2022

Document Version
Accepted author manuscript, peer reviewed version

Multi-Energy Microgrids: An Optimal Dispatch Model for Water-Energy Nexus

Faezeh Jalilian[1], Mohammad Amin Mirzaei[1], Behnam Mohammadi-Ivatloo[1,3], Kazem Zare[1*], Mousa Marzband[2], Amjad Anvari-Moghaddam[3,1]

[1]Faculty of Electrical and Computer Engineering, University of Tabriz, Tabriz, Iran

[2]Northumbria University, Electrical Power and Control Systems Research Group, Ellison Place NE1 8ST Newcastle upon Tyne, United Kingdom

[3] Integrated Energy Systems Laboratory, Department of Energy Technology, Aalborg University, 9220 Aalborg, Denmark

Abstract:

The significant rising interest on distributed energy resource has influenced the global attention for the integration of multi-energy sources such as electric, gas, water heating, However, these resources inherent with internal and external uncertainties which impose challenges to system functionalities and efficiency. This paper proposes an integrated scheduling model for optimal dispatch of cooling, heating, power, gas and water sources in an energy-water microgrid. In fact the microgrid operator participates in the power, heat, and gas markets and utilize energy conversion facilities to obtain required demands. Further , the water and energy storage systems (WESSs) and demand response program (DRP) have defined the optimal scheduling of the combined cooling, heating, power, gas, and water-based microgrid. In addition, a multi-objective two-stage stochastic optimization problem is formulated to minimize the total cost, including operating cost and emission cost. It also considers the amount of water extracted from wells due to the uncertainties of power demand, wind power, and market price. Moreover,, the epsilon-constraint method and fuzzy satisfying approach have been applied to obtain the optimal solution in this multi-objective problem. Ultimately, the simulation results confirm the advantages of simultaneous consideration on WESSs and DRP for the total cost of the proposed energy-water microgrid.

Keywords: Energy-water nexus, multi-energy microgrid, energy storage systems, multi-objective optimization, two-stage stochastic programming, demand response program

Nomenclature:

Indices

t, τ	Time interval
j	CHP units
w	Scenario

Parameters

N_t	Total of period time
N_j	Total of CHP units
N_w	Total of scenarios
C_j^{su} / C_j^{sd}	Start-up/shut-down cost of CHP units ($/kWh)
$C^{EL,dn} / C^{EL,up}$	Increase/decrease cost of electrical demand ($/kWh)
DRE	Adjustable electrical load value (%)
ρ_w	Occurrence probability of scenario
$ED_{t,w}$	Electrical demand (kW)
$HD_t / GD_t / CD_t / WD_t$	Heat/gas/cooling/water demand (kW)
$ED_{t,w}^{DR}$	The value of electrical demand after the applying DR program (kW)
$P_{t,w}^{wind}$	The power generated via wind turbine (kW)
$\lambda_{t,w}^{EM}$	Electricity market price ($/kWh)
λ_t^{HM}	Heat market price ($/kWh)
λ_t^{GM}	Gas market price ($/kWh)
λ^C	Carbon price ($/kg)
α, β, γ	Carbon emission coefficient (kg/kWh)
K	Positive constant
CS	Cross-section of WST (m^2)
$LS^{\max}$	Maximum capacity of WST (m)
L^{WL}	Level of Water well (m)
L^G	The height of WST (m)
g	Gravity (m^2/h)
φ	Water density (kg/m^3)
T_j^{ON} / T_j^{OFF}	Minimum on/off time of the CHP units (h)
η_j	The efficiency of CHP units
$H^{gb,\max} / H^{gb,\min}$	Max/min capacity of gas boiler (kW)
$H^{eb,\max} / H^{eb,\min}$	Max/min capacity of electric boiler (kW)
$E^{HS,\max} / E^{HS,\min}$	Max/min level of HSS (kWh)
$E^{HS,\mathrm{ch},\max} / E^{HS,\mathrm{disch},\max}$	Maximum charging/discharging of HSS (kW)
$E^{GS,\max} / E^{GS,\min}$	Max/min level of GSS (kWh)
$P^{ch,GS,\max} / P^{ch,GS,\min}$	Max/min charging of GSS (kW)
$P^{disch,GS,\max} / P^{disch,GS,\min}$	Max/min discharging of GSS (kW)

$E^{ES,\max} / E^{ES,\min}$	Max/min level of ESS (kWh)
$P^{ch,ES,\max} / P^{ch,ES,\min}$	Max/min charging of ESS (kW)
$P^{disch,ES,\max} / P^{disch,ES,\min}$	Max/min discharging of ESS (kW)
$E^{ISS,\max} / E^{ISS,\min}$	Max/min level of ISS (kWh)
$P^{ch,ISS,\max} / P^{ch,ISS,\min}$	Max/min charging of ISS (kW)
$P^{disch,ISS,\max} / P^{disch,ISS,\min}$	Max/min discharging of ISS (kW)
$C^{abchlr,\max} / C^{abchlr,\min}$	Max/min capacity of absorption chiller (kW)
$Q^{S,ch,\max} / Q^{S,disch,\max}$	Maximum charging/discharging of WST (m^3/h)
$Q^{D,\max}$	Maximum capacity of SDS (m^3/h)
η^{gb}	The efficiency of gas boiler
η^{eb}	The efficiency of electrical boiler
η^{HS}	The efficiency of HSS
$\eta^{HS,ch} / \eta^{HS,disch}$	The efficiency of charging/discharging HSS
$\eta^{ch,GS} / \eta^{disch,GS}$	The efficiency of charging/discharging GSS
$\eta^{ch,ES} / \eta^{disch,ES}$	The efficiency of charging/discharging ESS
$\eta^{ch,ISS} / \eta^{disch,ISS}$	The efficiency of charging/discharging ISS
η^{abchlr}	The efficiency of absorption chiller
η^{PWL}	The efficiency of water well pump
η^{PS}	The efficiency of WST pump
η^{D}	The efficiency of SDS

Variables

$dr_{t,w}^{EL,up}, dr_{t,w}^{EL,dn}$	Changes of the electrical demand after applying the demand response program (kW)
$P_{t,w}^{EM,imp} / P_{t,w}^{EM,sell}$	Imported/sold power from/to the main grid (kW)
$P_{t,w}^{HM,imp} / P_{t,w}^{HM,sell}$	Imported/sold heat from/to the main grid (kW)
$P_{t,w}^{GM,imp}$	Imported gas from the main grid (kW)
$P_{t,w,j}$	The power generated via CHP units (kW)
$H_{t,w,j}$	The heat generated via CHP units (kW)
$GC_{t,w,j}$	Gas consumed via CHP units (kW)
$GB_{t,w}^{gb}$	Gas consumed via gas boiler (kW)
$H_{t,w}^{gb}$	The heat generated via gas boiler (kW)
$EB_{t,w}^{eb}$	Power consumed via electric boiler (kW)
$H_{t,w}^{eb}$	The heat generated via electric boiler (kW)
$E_{t,w}^{HS}$	Charge level of HSS (kWh)
$E_{t,w}^{GS}$	Charge level of GSS (kWh)

$E_{t,w}^{ES}$	Charge level of ESS (kWh)
$E_{t,w}^{ISS}$	Charge level of ISS (kWh)
$H_{t,w}^{HS,ch}$ / $H_{t,w}^{HS,disch}$	Charging/discharging of the HSS *w* (kW)
$P_{t,w}^{ch,GS}$ / $P_{t,w}^{disch,GS}$	Charging/discharging of the GSS (kW)
$P_{t,w}^{ch,ES}$ / $P_{t,w}^{disch,ES}$	Charging/discharging of the ESS (kW)
$P_{t,w}^{ch,ISS}$ / $P_{t,w}^{disch,ISS}$	Charging/discharging of the ISS (kW)
$C_{t,w}^{abchlr}$	The cooling generated by absorption chiller (kW)
$H_{t,w}^{abchlr}$	Heat consumed by absorption chiller (kW)
$Q_{t,w}^{WL}$	Water extracted from the well (m^3/h)
$Q_{t,w}^{D}$	Water generation by SDS (m^3/h)
$Q_{t,w}^{S,ch}$ / $Q_{t,w}^{S,disch}$	Charging/discharging amount of WST (m^3/h)
$LS_{t,w}$	The water level of WST (m)
$P_{t,w}^{PWL}$	Power consumed by water well pump (kW)
$P_{t,w}^{PS}$	Power consumed by WST pump (kW)
$P_{t,w}^{D}$	Power consumed by SDS (kW)
$P_{t,w}^{water}$	Total power consumed by water network (kW)

Binary variables

$\mathrm{I}_{t,j}$	On/off state of the CHP units
$V_{1,t}$ / $V_{2,t}$	Operating point status of the second type CHP unit in the first/second convex sector of FOR
$Y_{t,j}$ / $Z_{t,j}$	Start-up/shut-down of CHP units
$I_{t,w}^{gb}$	On/off state of the gas boiler
$I_{t,w}^{eb}$	On/off state of the electric boiler
$I_{t,w}^{HS,ch}$ / $I_{t,w}^{HS,disch}$	Charging/discharging state of HSS
$I_{t,w}^{ch,GS}$ / $I_{t,w}^{disch,GS}$	Charging/discharging state of GSS
$I_{t,w}^{ch,ES}$ / $I_{t,w}^{disch,ES}$	Charging/discharging state of ESS
$I_{t,w}^{ch,ISS}$ / $I_{t,w}^{disch,ISS}$	Charging/discharging state of ISS
$I_{t,w}^{S,ch}$ / $I_{t,w}^{S,disch}$	Charging/discharging state of WST

1. Introduction

1.1. Overview

In recent years, due to problems such as scarcity of conventional energy resources and the aging of the electricity network infrastructure, the power system has faced challenges. Generating power and

supplying different loads through locally available renewable energy sources (RESs) have led to the emergence of a new concept called microgrid. The microgrid is a small-scale power system that can provide consumers' energy and works in both islanded and grid-connected modes (Hemmati et al., 2018; Mansour-Saatloo et al., 2020b). With the integration of multi-energy sources into a microgrid, such as boilers, combined heat and power (CHP) units and chillers, multi-energy microgrids (MEMGs) can be formed. This structure has advantages such as mitigating greenhouse gas emissions, reducing costs and increasing efficiency through leveraging an integrated energy system model. The MEMG can meet thermal, electrical and cooling loads simultaneously (Mansour-Saatloo et al., 2020b; Pourghasem et al., 2019). Co-/tri-generation systems in MEMG can increase power generation by about 30% in power plants, while reducing greenhouse gas emission by approximately 13-18%, which denote the economic and environmental benefits of such energy sources (Wu et al., 2017). On the other hand, economic development together with rapid population growth and urbanization significantly affect vital resources, such as water and energy. The water and energy crisis is one of the critical problems in the future with increasing demand, increasing scales, climate change and natural disasters (Dai et al., 2018). According to statistics, energy and water demands will grow by about 40% and 30%, respectively, by 2035 (Li et al., 2019). Water and energy systems are inextricably interdependent. Water can be used to produce and consume energy in different stages, while energy can be used to extract, deliver, distribute, and treat water (Shang et al., 2018). Thus, to enable an efficient energy-water nexus, integrated approaches can be used to scheduling and operate water and energy systems through the so-called energy-water microgrids (EWMG) (Moazeni and Khazaei, 2020a).

1.2. Literature review

Many studies have evaluated the optimal scheduling and management of microgrids in both (grid-connected and islanded) modes. A bidding strategy for microgrids has been presented in (Mirzaei et al., 2020a) using a two-stage bi-level approach to their participation in different markets, where the capability to reconfiguration microgrids is considered to maximize microgrid profit. A novel index for reconfigurable microgrids islanding operation has been introduced in (Hemmati et al., 2020), which is called the probability of islanding operation and represents the ability of the microgrid to meet load

demand, where chance-constrained scheduling for the reconfigurable microgrid is presented in order to minimize the costs. In (Daneshvar et al., 2020) various models for microgrids participation in the energy trading market have been proposed by considering a transactive energy framework to handle energy exchange in the network and in the presence of uncertainties. The decision-making structure of active distribution networks (includes retailers and microgrids) has been presented as a bi-level approach in (Fateh et al., 2020), in which through a proposed structure for energy exchange with the market, retailers and microgrids can optimize related goals. In (Hou et al., 2020), a multi-objective approach for microgrid economic operation with electric vehicles, shiftable loads and generators has been introduced, where the operating cost of the microgrid, utilization rate of photovoltaic energy and the power oscillation between the microgrid and the main network are considered as objectives. The optimization of power exchanging in reconfigurable microgrids by considering distributed energy resources has been investigated in (Jahani et al., 2021).

Besides the microgrids problem, the concept of the MEMGs has attracted much attention, so that researchers have investigated it under different approaches. An optimal multi-objective problem for multi-carrier microgrids energy management has been employed in (Murty and Kumar, 2020) in order to minimize cost and reduce losses and emissions, where two grid-connected and stand-alone operating modes are proposed for the microgrid. A stochastic-robust approach has been optimized for combined cooling, heating and power-based (CCHP) microgrids in (Wang, Y. et al., 2020) to coordinate the optimization of CCHP microgrids operation and power exchange with the electricity market under existing uncertainties. Authors of (Cui et al., 2020) have focused on the importance and effects of modelling devices for the multi-objective optimal planning of CCHP-based microgrids and shiftable load using a partial load ratio model. Optimal scheduling of MEMG integrated with RESs has been investigated in (Saberi et al., 2019) to solve economic and environmental problems, in which real-time demand response (DR) is considered. In (Amir and Azimian, 2020), dynamic MEMGs development has been analyzed using a long-term dynamic MEMGs scheduling model under existing uncertainties. Authors of (Ding et al., 2021) have focused on the economic and environmental evaluation of MEMGs under a hybrid robust/stochastic optimization approach to minimize energy cost and CO_2 emission rate.

A temporally-coordinated approach for MEMG taking into account various energy properties has been represented in (Li and Xu, 2019) to coordinate diverse energies in the presence of uncertainties from RESs, electrical load, and prices. In (Mansour-Saatloo et al., 2020a), the authors have focused on the concept of CHP-based microgrid by considering the integrated DR and hydrogen storage system. An integration structure of combined cooling, heating, power and gas-based (CCHPG) microgrid has been investigated in (Yang et al., 2020) to manage risk by considering operating cost control. In (Nami et al., 2020), the waste heat and geothermal heat resources have been utilized in CCHP units to supply thermal and electrical demands, in which not only is provided energy demands but also surplus energy is delivered to the main grid. A scenario-based stochastic isolated MEMGs investment programming model has been introduced in (Ehsan and Yang, 2019) to minimize costs and emission under different uncertainties and demands. Likewise, the multi-period programming problem of MEMG has been studied in (Wei et al., 2020a) taking into account long-term and short-term uncertainties.

Significant studies have also been done in the field of integrated water and energy systems and their optimal management. In (Pakdel et al., 2020), a multi-objective optimization approach has been introduced to reduce costs and groundwater extraction, in which the concept of transactive energy is used to achieve further system flexibility. In (Ahmadi et al., 2020), an integrated scheduling structure for supplying sustainable water and energy has been presented, where a novel model is applied to investigate synergies and conflicts of the scheduling of both the energy and water systems simultaneously. An optimization method for minimizing energy usage of the water network with fixed and variable speed pumps in the EWMG system has been demonstrated in (Moazeni and Khazaei, 2020b). A navel approach has been proposed in (Feizizadeh et al., 2021) in order to sustainability evaluation of urban drinking water consumption patterns in Tabriz city, where urban structure and population have a significant effect on water consumption. A comprehensive programming model consists of one main problem, and two sub-problems have been proposed to develop the resilience of power-water distribution networks with microgrids, where the aim of the main problem is to minimize the investment costs and the expected load's unavailability to power and water against storms (Najafi et al., 2019). In (Roustaei et al., 2020), a scenario-based management structure for EWMG to maintain

the balance of different energy carriers and optimal programming for its infrastructure has been provided, where according to this programming, the total investment costs and costs of environmental pollutants are minimized. A co-optimization approach of the islanded micro water-energy system has been used to minimize energy usage in water systems and to minimize the cost of energy production at the energy system on a daily basis (Moazeni et al., 2020). By using an environment-based input-output approach, the authors of (Wang, X.-C. et al., 2020) have explored water-energy nexus while considering carbon emissions. In (Zhang et al., 2020), a novel strategy has introduced to integrate the emerging and existing renewable energy resources into a community MG to improve community resilience, where an energy-water nexus model has been presented for sustainable system development.

The contribution of the extended water-energy nexus (e.g. food, pollution, ground, waste and so on) to improve the environmental sustainability has critically discussed in (Wang et al.2021).. In (Sui et al., 2021), the optimal management structure has been proposed with the integration of a MG and a water supply system to mitigate the problem of the water system fluctuation Two optimal models for a water-energy system have observed in (Moazeni and Khazaei, 2021), which is to provide the optimal number and location of pumps-as-turbines by one model, and to minimize the energy production cost by other model, to investigate the impact of demand response on the energy storing of the water-energy network. Authors in (Li et al., 2018) have presented the water system capacity to supply DR program management to the power network with respect to the micro water-energy nexus structure.

1.3. Contribution

Based on the reviewed literature and the authors' best knowledge, the focus on combined cooling, heating, power, gas, and water-based microgrid (CCHPGW-MG) has been ignored. The most research gaps of the reviewed literature as follow:

- Some literature has only considered the optimal management and scheduling of microgrids e.g. (Daneshvar et al., 2020; Fateh et al., 2020; Hemmati et al., 2020; Hou et al., 2020; Jahani et al., 2021; Mirzaei et al., 2020a) and has ignored the effect of multi-energy microgrids, even though it is one of the essential research aspects.

- Numerous studies have been investigated the impacts and benefits of the multi-energy microgrids in different approaches e.g. (Ding et al., 2021; Ehsan and Yang, 2019; Murty and Kumar, 2020; Nami et al., 2020; Saberi et al., 2019; Wei et al., 2020b), while disregarding the effect of energy-water microgrids. Nevertheless, the energy-water microgrids should gain the prime attention because of the energy and water crisis.
- Most of the literature has observed only on energy-water microgrids planning, e.g. (Moazeni and Khazaei, 2020b; Moazeni et al., 2020; Roustaei et al., 2020; Wang et al., 2021; Zhang et al., 2020), while ignoring the optimal integrated scheduling of the energy-water microgrids to supply different demands.

Table 1 shows a comparison of the existing models in the reviewed literature with the proposed one in this study. As can be clearly observed, this paper presents a developed microgrid model under the concept of CCHPGW-MG, which meets different energy demands simultaneously via participating in multi-energy markets. The proposed model is formulated as a multi-objective optimization problem, which aims to minimize operating cost, emission cost, and the amount of potable water extracted from water wells, simultaneously. The ε-constraint method is employed to solve the multi-objective problem, and the fuzzy approach is also used to select the optimal values of the objective functions. Furthermore, the DR program is considered to shift electrical loads from peak hours to off-peak hours and reduce total operating cost. A two-stage stochastic scheduling approach is also applied to manage uncertainties. The main contributions of this study can be categorized as follows:

- An energy-water microgrid is introduced in this paper under the concept of CCHPGW-MG, in which the microgrid operator can participate in multi-energy markets to supply different demands, including electricity, heating, cooling, gas and water.
- The effect of multiple storage systems, including heat storage system (HSS), electrical storage system (ESS), gas storage system (GSS), ice storage system (ISS), and water storage tank (WST), as well as DR program, is investigated on optimal scheduling of the proposed microgrid.
- Water system technologies, including seawater desalination system (SDS), well water and WST, is considered to supply water demand and increase water system flexibility.

- A two-stage stochastic approach is adopted to manage the uncertainties associated with electrical load, wind power and electricity price in the multi-energy microgrid.

The rest of the paper is organized as follows: The structure of the CCHPGW-MG along with its details is given in Section 2. Section 3 introduces the problem formulation including the objective functions, problem constraints, and the examined multi-objective optimization model. Simulation results are given in Section 4. Finally, Section 5 concludes the paper.

Table 1: Comparison of reviewed literature with the current work

Ref	Multi-energy MG			EWMG	Demand response	Objective functions			Uncertainty modeling
	CHP	CCHP	CCHPG			Energy cost	Emission cost	Water well	
(Mirzaei et al., 2020a)					✓	✓			Stochastic-Information gap decision theory
(Wang, Y. et al., 2020)		✓				✓			Stochastic -robust, conditional value-at-risk (CVaR)
(Cui et al., 2020)		✓			✓	✓	✓		-
(Amir and Azimian, 2020)	✓				✓	✓	✓		Two-stage stochastic
(Mansour-Saatloo et al., 2020a)	✓				✓	✓			Robust
(Yang et al., 2020)			✓			✓			Stochastic-robust
(Ehsan and Yang, 2019)		✓				✓	✓		Scenario-based stochastic
(Moazeni and Khazaei, 2020b)				✓		✓			-
(Roustaei et al., 2020)	✓			✓		✓	✓		Scenario-based stochastic
(Zhang et al., 2020)				✓		✓	✓		-
(Sui et al., 2021)				✓		✓			-
Proposed model			✓	✓	✓	✓	✓	✓	Two-stage stochastic

2. Structure of CCHPGW-MG

Fig.1 shows the structure of the CCHPGW-MG, energy sector technologies including electrical boiler, gas boiler, two types of CHP unit with different feasible operating regions (FORs), wind turbines, heat storage system (HSS), electrical storage system (ESS), gas storage system (GSS), ice storage system

(ISS), absorption chiller and water sector technologies including seawater desalination system (SDS), water storage tank (WST) and well water. In this study, a two-stage stochastic approach is applied to handle uncertainties related to the electrical load, wind power, and electricity price in the proposed model. The first stage is associated with the start-up and shut-down costs of the CHP units, and the second stage corresponds to the scenarios related to the costs of operation and distribution of the energy and water systems technologies. The microgrid is fed by the upstream electricity, gas and heating networks, wind turbines, and water to meet various energy and water demands securely. As mentioned before, the water and energy crisis is one of the fundamental problems which has led researchers to investigate. The use of desalination technology solves the water shortage issue, but since eliminating salt from seawater consumes a lot of energy, so using this technology alone is not cost-effective. In addition, the reduction of groundwater freshwater reserves is another major problem. Therefore, simultaneous consideration of water system technologies such as SDS, WST, and water wells is a fundamental solution to solve the water and energy crisis.

- **Electrical sector:** According to Fig.1, electricity demand, equipment input such as electrical boiler, ISS and water sector technologies is met by the upstream electricity network, CHP units, ESS and wind turbines. Furthermore, part of the power generated, in the hours when the electricity market price is high, sold to the electricity network.
- **Heat sector:** Heat demand and absorption chiller input is supplied by the upstream heating network, CHP units, electrical boiler, gas boiler and HSS. Furthermore, part of the heat produced during heating market high-price periods is sold to the heating network.
- **Gas sector**: Gas load, the input of CHP units and gas boiler is fulfilled by the upstream gas network and GSS.
- **Cooling sector**: Cooling demand is provided by the ISS and absorption chiller.
- **Water sector**: Water system technologies include SDS, WST and well water, meet water demand by consuming electricity.

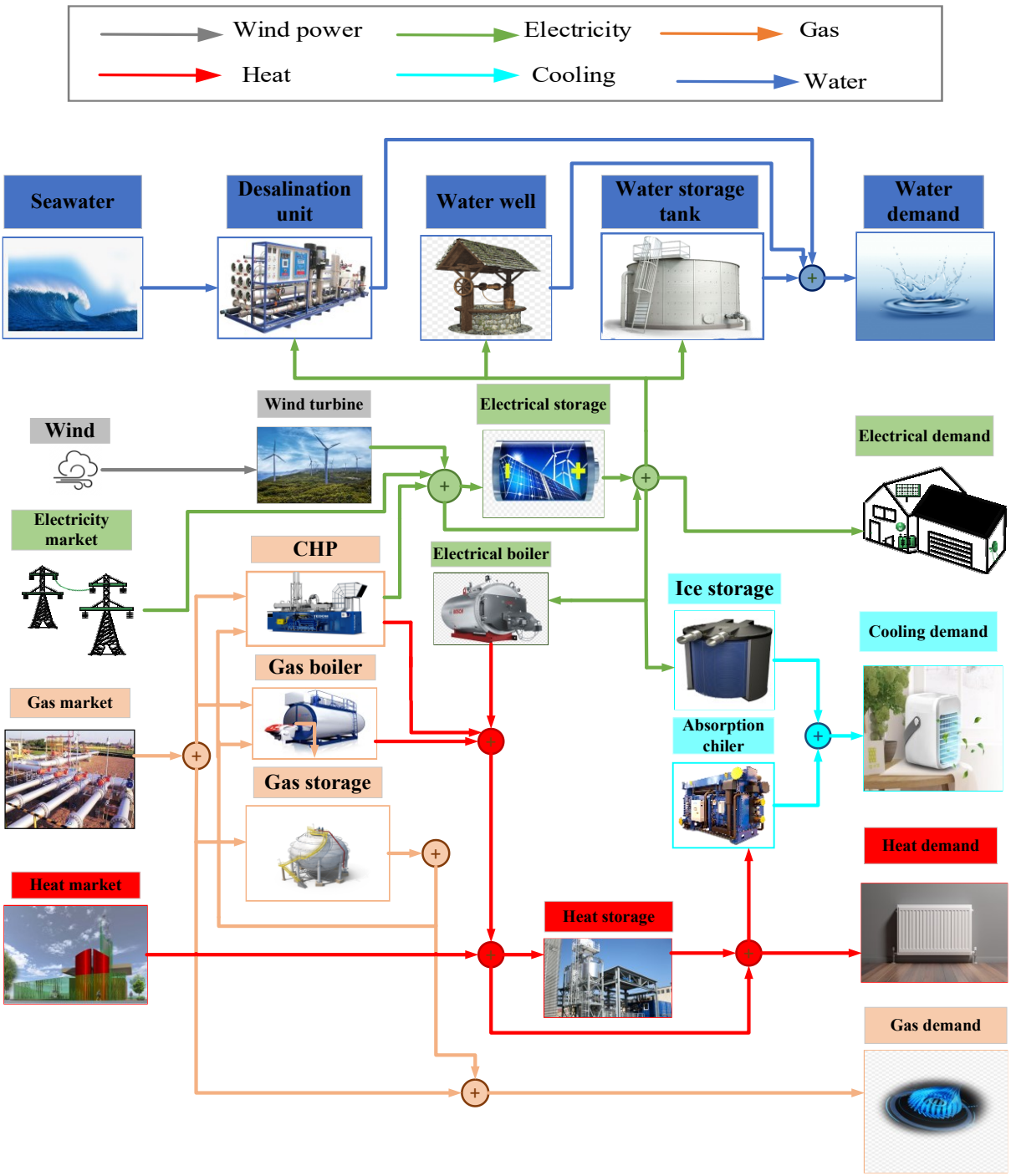

Fig.1. Structure of the CCHPGW-MG

3. Problem formulation

The problem formulation of the CCHPGW-MG, including the objective function and constraints associated with both energy and water systems and the ε-constraint method, is given in this section.

3.1. Objective function:

This paper aims to minimize the total cost, including operating cost and emission cost, and the amount of potable water extracted from the water well during 24 hours period. The first objective is to minimise the total system costs, where cost ^{O} is the operating cost and cost ^{E} is the emissions cost, as shown in equation (1). In equation (2), according to the two-stage stochastic approach in the problem, the first and second term is associated with the start-up and shut-down costs of the CHP units in the first stage, respectively. The second stage is related to the costs of operation and dispatch of the integrated system that includes the third to ninth terms. The third and fourth term demonstrates cost and the revenue obtained from purchasing/selling electricity from/to the main electricity network. The fifth and sixth term denotes cost and revenue to obtained from purchasing/selling heat from/to the main heating network. The seventh term is associated with the cost of gas purchased from the main gas network. Finally, the eighth and ninth term is related to the cost of the electricity DR program. The emissions cost is expressed using equation equation (3), in which the first, second, and third terms are the carbon emission costs associated with electricity, heat, and gas purchased from the main grid, respectively. The second objective is to minimise the extracted potable water volume from the well, which is demonstrated in equation (4).

$$\text{Cost} = \text{cost}^{O} + \text{cost}^{E} \tag{1}$$

$$\text{Cost}^{O} = \min \sum_{j=1}^{N_j} \sum_{t=1}^{N_t} (C_j^{su} Y_{t,j} + C_j^{sd} Z_{t,j}) + \sum_{w=1}^{N_w} \rho_w \sum_{t=1}^{N_t} \begin{bmatrix} \lambda_{t,w}^{EM} P_{t,w}^{EM,imp} - \lambda_{t,w}^{EM} P_{t,w}^{EM,sell} \\ +\lambda_t^{HM} P_{t,w}^{HM,imp} - \lambda_t^{HM} P_{t,w}^{HM,sell} \\ +\lambda_t^{GM} P_{t,w}^{GM,imp} \\ +C^{EL,up} dr_{t,w}^{EL,up} + C^{EL,dn} dr_{t,w}^{EL,dn} \end{bmatrix} \tag{2}$$

$$\text{Cost}^{E} = \min \sum_{w=1}^{N_w} \rho_w \sum_{t=1}^{N_t} [(\alpha P_{t,w}^{EM,imp} + \beta P_{t,w}^{HM,imp} + \gamma P_{t,w}^{GM,imp}) \lambda^{C}] \tag{3}$$

$$\text{Water} = \min \sum_{w=1}^{N_w} \rho_w \sum_{t=1}^{N_t} [Q_{t,w}^{WL}] \tag{4}$$

3.2. CHP units constraints:

Based on the essence of the cogeneration units, the generated heat and power by the CHP units are interdependent. To demonstrate this dependence, a feasible operating region (FOR) is considered for each CHP unit. In this paper, the two types of CHP units the first and second type are considered with convex and non-convex FORs, respectively. Thus, each CHP unit must be operated in its feasible

region, which is shown in Fig. 2. The mathematical model and the investigation of both the types of the CHP units have obtained from reference (Hadayeghparast et al., 2019). Equations (5)-(9) are utilized to the first type of CHP unit. The presented convex FOR is modelled by the (5)-(7) equations. Besides, the limitations of the generated heat and power by the CHP unit are presented in equations (8) and (9), respectively.

$$P_{t,w,j1} - P_{j1}^{A} - \frac{P_{j1}^{A} - P_{j1}^{B}}{H_{j1}^{A} - H_{j1}^{B}} \times (H_{t,w,j1} - H_{j1}^{A}) \le 0 \tag{5}$$

$$P_{t,w,j1} - P_{j1}^{B} - \frac{P_{j1}^{B} - P_{j1}^{C}}{H_{j1}^{B} - H_{j1}^{C}} \times (H_{t,w,j1} - H_{j1}^{B}) \ge -(1 - \mathrm{I}_{t,j}) \times K \tag{6}$$

$$P_{t,w,j1} - P_{j1}^{C} - \frac{P_{j1}^{C} - P_{j1}^{D}}{H_{j1}^{C} - H_{j1}^{D}} \times (H_{t,w,j1} - H_{j1}^{C}) \ge -(1 - \mathrm{I}_{t,j}) \times K \tag{7}$$

$$0 \le H_{t,w,j1} \le H_{j1}^{B} \times \mathrm{I}_{t,j} \tag{8}$$

$$0 \le P_{t,w,j1} \le P_{j1}^{A} \times \mathrm{I}_{t,j} \tag{9}$$

Equations (10)-(18) are used for the second type of CHP unit. Since the second type CHP has a non-convex FOR, its formulation is different from the first type CHP with convex FOR. Hence, in the formulation structure of the second type CHP, two additional binary variables $V_{1,t}$ and $V_{2,t}$ are used. Therefore, the non-convex FOR is divided into two convex subsections (a) and (b), as demonstrated in Fig. 2. The presented FOR for the second type of CHP is modelled by the (10)-(13) equations. Equations (14) and (15) represent the maximum of the generated power and heat by the CHP unit, respectively. In equations (16)-(18), the binary variables $V_{1,t}$ and $V_{2,t}$ are utilized to determine the sector where the operating point of the CHP unit is located. Equation (16) illustrates, which when the CHP unit is ON, the operating sector of this unit would be either (a) [$V_{1,t}$ = 1, $V_{2,t}$ = 0] or (b) [$V_{1,t}$ = 0, $V_{2,t}$ = 1].

$$P_{t,w,j2} - P_{j2}^{B} - \frac{P_{j2}^{B} - P_{j2}^{C}}{H_{j2}^{B} - H_{j2}^{C}} \times (H_{t,w,j2} - H_{j2}^{B}) \le 0 \tag{10}$$

$$P_{t,w,j2} - P_{j2}^{C} - \frac{P_{j2}^{C} - P_{j2}^{D}}{H_{j2}^{C} - H_{j2}^{D}} \times (H_{t,w,j2} - H_{j2}^{C}) \ge 0 \tag{11}$$

$$P_{t,w,j2} - P_{j2}^{E} - \frac{P_{j2}^{E} - P_{j2}^{F}}{H_{j2}^{E} - H_{j2}^{F}} \times (H_{t,w,j2} - H_{j2}^{E}) \ge -(1 - V_{1,t}) \times K \tag{12}$$

$$P_{t,w,j2} - P_{j2}^{D} - \frac{P_{j2}^{D} - P_{j2}^{E}}{H_{j2}^{D} - H_{j2}^{E}} \times (H_{t,w,j2} - H_{j2}^{D}) \ge -(1 - V_{2,t}) \times K \tag{13}$$

$$0 \le P_{t,w,j2} \le P_{j2}^{A} \times I_{t,j} \quad (14)$$

$$0 \le H_{t,w,j2} \le H_{j2}^{C} \times I_{t,j} \quad (15)$$

$$V_{1,t} + V_{2,t} = I_{t,j} \quad (16)$$

$$H_{t,w,j2} - H_{j2}^{E} \le (1 - V_{1,t}) \times K \quad (17)$$

$$H_{t,w,j2} - H_{j2}^{E} \ge -(1 - V_{2,t}) \times K \quad (18)$$

Equation (19) expresses the relation between the binary variables of CHP units. Equations (20)-(21) illustrate the minimum up/down time constraints of the CHP units, respectively (Zhou et al., 2019).

$$I_{t,j} - I_{t-1,j} = Y_{t,j} - Z_{t,j} \quad (19)$$

$$I_{\tau,j} \ge Y_{t,j} \qquad \forall t \le \tau \le t + T_j^{ON} - 1 \quad (20)$$

$$1 - I_{\tau,j} \ge Z_{t,j} \quad \forall t \le \tau \le t + T_j^{OFF} - 1 \quad (21)$$

Equation (22) shows the amount of natural gas consumed via CHP units (Mirzaei et al., 2020c).

$$GC_{t,w,j} = \frac{P_{t,w,j}}{\eta_j} + SU_{t,j} + SD_{t,j} \quad (22)$$

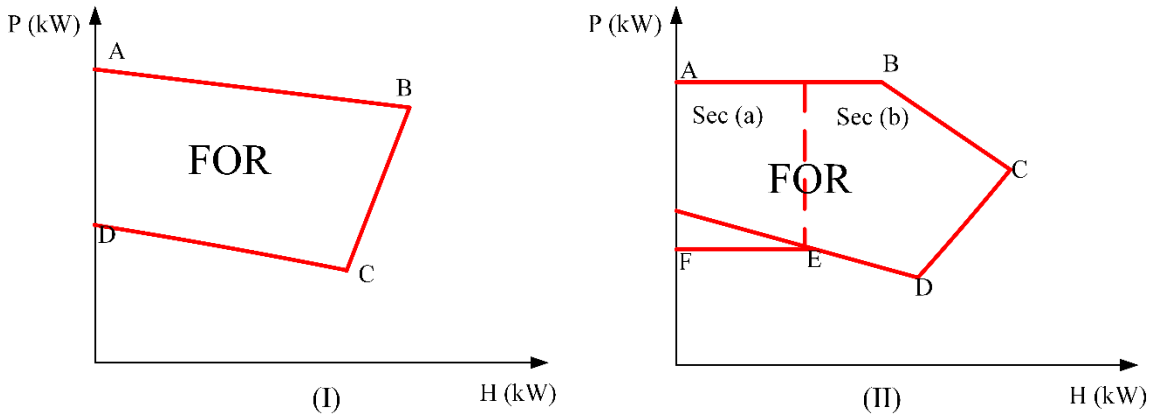

Fig. 2. FOR for CHP units (I) first type, (II) second type

3.3. Gas boiler constraints:

A gas boiler is a device, which generates heat using natural gas. The amount of natural gas used by the gas boiler and the heat generated by it are expressed in equation (23). Also, the amount of maximum and minimum heat generated by the gas boiler is defined by equation (24) (Mansour-Saatloo et al., 2020b).

$$GB_{t,w}^{gb} = \frac{H_{t,w}^{gb}}{\eta^{gb}} \quad (23)$$

$$H^{gb,\min} \times I_{t,w}^{gb} \le H_{t,w}^{gb} \le H^{gb,\max} \times I_{t,w}^{gb} \quad (24)$$

3.4. Electric boiler constraints:

The electric boiler generates heat by consuming electricity. The amount of electricity consumed by the electric boiler and the heat generated by it is demonstrated at time *t* and scenario *w*, in equation (25). Also, the amount of maximum and minimum heat generated by the electric boiler is calculated by equation (26), at time *t* and scenario *w*.

$$EB_{t,w}^{eb} = \frac{H_{t,w}^{eb}}{\eta^{eb}} \tag{25}$$

$$H^{eb,\min} \times I_{t,w}^{eb} \le H_{t,w}^{eb} \le H^{eb,\max} \times I_{t,w}^{eb} \tag{26}$$

3.5. Heat storage system constraints:

The reserved heat in the HSS at time *t* and scenario *w* is determined by equation (27). According to equation (28), the reserved heat is limited between the minimum and maximum reservoir capacity. Furthermore, the limitations of charging/discharging rates are illustrated in equations (29) and (30), respectively. Finally, equation (31) states which the HSS cannot be charged and discharged, simultaneously (Mansour-Saatloo et al., 2020a).

$$E_{t,w}^{HS} = (1-\eta^{HS})E_{t-1,w}^{HS} + \eta^{HS,ch}H_{t,w}^{HS,ch} - \frac{H_{t,w}^{HS,disch}}{\eta^{HS,disch}} \tag{27}$$

$$E^{HS,\min} \le E_{t,w}^{HS} \le E^{HS,\max} \tag{28}$$

$$E_{t,w}^{HS} - E_{t-1,w}^{HS} \le E^{HS,\mathrm{ch},\max} \tag{29}$$

$$E_{t-1,w}^{HS} - E_{t,w}^{HS} \le E^{HS,\mathrm{disch},\max} \tag{30}$$

$$I_{t,w}^{HS,ch} + I_{t,w}^{HS,disch} \le 1 \tag{31}$$

3.6. Gas storage system constraints:

Similar to the HSS, the amount of stored gas in the GSS at time *t* and scenario *w* is expressed in equation (32) and limited by equation (33). In addition, GSS charging/discharging rates are limited via equations (34) and (35), respectively. Equation (36) prevents the simultaneous occurrence of charge and discharge rates (Mansour-Saatloo et al., 2020a).

$$E_{t,w}^{GS} = E_{t-1,w}^{GS} + (\eta^{ch,\mathrm{GS}} \times P_{t,w}^{ch,\mathrm{GS}} - \frac{P_{t,w}^{disch,\mathrm{GS}}}{\eta^{disch,\mathrm{GS}}}) \times \Delta t \tag{32}$$

$$E^{GS,\min} \le E_{t,w}^{GS} \le E^{GS,\max} \tag{33}$$

$$P^{ch,\mathrm{GS},\min} I_{t,w}^{ch,\mathrm{GS}} \le P_{t,w}^{ch,\mathrm{GS}} \le P^{ch,\mathrm{GS},\max} I_{t,w}^{ch,\mathrm{GS}} \tag{34}$$

$$P^{disch,\mathrm{GS},\min} I_{t,w}^{disch,\mathrm{GS}} \le P_{t,w}^{disch,\mathrm{GS}} \le P^{disch,\mathrm{GS},\max} I_{t,w}^{disch,\mathrm{GS}} \tag{35}$$

$$I_{t,w}^{ch,\mathrm{GS}} + I_{t,w}^{disch,\mathrm{GS}} \le 1 \tag{36}$$

3.7. Electrical storage system constraints:

Similar to the two storage systems mentioned above, the amount of stored electrical in the ESS at time t and scenario w is expressed in equation (37) and limited by equation (38). Furthermore, ESS charging/discharging modes are limited via equations (39) and (40), respectively. Finally, equation (41) ensures which ESS cannot be charged and discharged simultaneously (Mansour-Saatloo et al., 2020a).

$$E_{t,w}^{ES} = E_{t-1,w}^{ES} + (\eta^{ch,ES} \times P_{t,w}^{ch,ES} - \frac{P_{t,w}^{disch,ES}}{\eta^{disch,ES}}) \times \Delta t \quad (37)$$

$$E^{ES,\min} \le E_{t,w}^{ES} \le E^{ES,\max} \quad (38)$$

$$P^{ch,ES,\min} I_{t,w}^{ch,ES} \le P_{t,w}^{ch,ES} \le P^{ch,ES,\max} I_{t,w}^{ch,ES} \quad (39)$$

$$P^{disch,ES,\min} I_{t,w}^{disch,ES} \le P_{t,w}^{disch,ES} \le P^{disch,ES,\max} I_{t,w}^{disch,ES} \quad (40)$$

$$I_{t,w}^{ch,ES} + I_{t,w}^{disch,ES} \le 1 \quad (41)$$

3.8. Ice storage system constraints:

The ISS is a type of storage system, which can meet the cooling demand by consuming electricity. The ISS level is presented at time t and scenario w, in equation (42) and limited by equation (43). Also, the limitations of charging/discharging rates are expressed in equations (44) and (45), respectively. Equation (46) prevents the simultaneous occurrence of charge and discharge rates (Mansour-Saatloo et al., 2020b).

$$E_{t,w}^{ISS} = E_{t-1,w}^{ISS} + (\eta^{ch,ISS} \times P_{t,w}^{ch,ISS} - \frac{P_{t,w}^{disch,ISS}}{\eta^{disch,ISS}}) \times \Delta t \quad (42)$$

$$E^{ISS,\min} \le E_{t,w}^{ISS} \le E^{ISS,\max} \quad (43)$$

$$P^{ch,ISS,\min} I_{t,w}^{ch,ISS} \le P_{t,w}^{ch,ISS} \le P^{ch,ISS,\max} I_{t,w}^{ch,ISS} \quad (44)$$

$$P^{disch,ISS,\min} I_{t,w}^{disch,ISS} \le P_{t,w}^{disch,ISS} \le P^{disch,ISS,\max} I_{t,w}^{disch,ISS} \quad (45)$$

$$I_{t,w}^{ch,ISS} + I_{t,w}^{disch,ISS} \le 1 \quad (46)$$

3.9. Absorption chiller:

The absorption chiller is a device which by using thermal energy to meet the cooling demand. Equation (47) demonstrates the amount of generated cooling energy by the absorption chiller at time t and scenario w, and is limited by equation (48) (Mansour-Saatloo et al., 2020b).

$$C_{t,w}^{abchlr} = H_{t,w}^{abchlr} \times \eta^{abchlr} \quad (47)$$

$$C^{abchlr,\min} \le C_{t,w}^{abchlr} \le C^{abchlr,\max} \quad (48)$$

3.10. Electrical demand response:

Electrical demand response program is one of the effective methods to handle electrical demands. Accordingly, electrical demands are shifted from peak hours to off-peak hours. Equations (49) and (50) represents the limitation of shiftable electrical demands at time *t* and scenario *w*. Equation (51) illustrate total shifted demands should be equal to total curtailed demands. Finally, after applying electrical demand response, total electrical demand is given via equation (52) (Mansour-Saatloo et al., 2020b).

$$0 \le dr_{t,w}^{EL,up} \le DRE \times ED_{t,w} \tag{49}$$

$$0 \le dr_{t,w}^{EL,\mathrm{dn}} \le DRE \times ED_{t,w} \tag{50}$$

$$\sum_{t=1}^{N_t} dr_{t,w}^{EL,up} = \sum_{t=1}^{N_t} dr_{t,w}^{EL,\mathrm{dn}} \tag{51}$$

$$ED_{t,w}^{DR} = ED_{t,w} + dr_{t,w}^{EL,up} - dr_{t,w}^{EL,\mathrm{dn}} \tag{52}$$

3.11. Water system model

In this section, the formulation of the water system is presented, which includes several components such as SDS, WST and water well. In this study is assumed which the WST pump consumes electricity when is in charge mode and the water well pump uses electricity when water is extracted from it, as well as the water level in the well is assumed to be constant due to the short optimization period (Pakdel et al., 2020). Equation (53) is the water balance constraint, which expresses that the obtained water from the SDS, WST and water well must be equal to the total water demand.

$$Q_{t,w}^{WL} + Q_{t,w}^{D} - Q_{t,w}^{S,ch} + Q_{t,w}^{S,disch} = WD_t \tag{53}$$

Water is pumped into the WST via the water source, such as a well or any other source, and the WST holds clean and excess water to meet the water demand for periods of low water. Equation (54) represents the water level in WST at time *t* and scenario *w*, which is limited by equation (55). Equations (56) and (57) shows the limitation of charge and discharge of the WST. Finally, equation (58) prevents simultaneous occurrence charging and discharging of the WST (Pakdel et al., 2020).

$$LS_{t,w} = LS_{t-1,w} + \frac{Q_{t,w}^{S,ch}}{CS} - \frac{Q_{t,w}^{S,disch}}{CS} \tag{54}$$

$$0 \le LS_{t,w} \le LS^{\max} \tag{55}$$

$$Q_{t,w}^{S,ch} \le Q^{S,ch,\max} I_{t,w}^{S,ch} \tag{56}$$

$$Q_{t,w}^{S,disch} \le Q^{S,disch,\max} I_{t,w}^{S,disch} \tag{57}$$

$$0 \le I_{t,w}^{S,ch} + I_{t,w}^{S,disch} \le 1 \tag{58}$$

Equations (59) and (60) show the power consumption by the water well pump and the WST pump at time *t* and scenario *w*, respectively. Also, 3.6×10^6 in the denominator of equations (59) and (60) is utilized to convert used power in the *W* range within 1 second to power consumption in the *kW* range within 1hour period (Pakdel et al., 2020).

$$P_{t,w}^{PWL} = Q_{t,w}^{WL} L^{WL} \frac{g\varphi}{\eta^{PWL}(3.6\times10^6)} \tag{59}$$

$$P_{t,w}^{PS} = Q_{t,w}^{S,ch}(LS_{t,w} + LS_{t-1,w} + L^G)\frac{g\varphi}{2\eta^{PS}(3.6\times10^6)} \tag{60}$$

The desalination unit consumes plenty of energy with respect to conventional water treatment methods. In particular , energy consumption for typical water treatment methods is around 0.06 kWh/m^3 , while the desalination unit energy consumption is varying between 0.5-16 kWh/m^3,depending on the unit type Desalination technologies are mainly categorized in to two type such as thermal processes and membrane processes. Thermal processes are deployed electrical and thermal energy for desalination, which the thermal and electrical energy requirement is fluctuating between 4-12 kWh/m^3 and 1.5-4 kWh/m^3, respectively. Membrane processes utilized only electrical power for desalination and the required energy is varying between 0.5-4 kWh/m^3. Membrane processes is deployed lower energy compared to the thermal processes, to prevent the evaporation of the seawater. The reverse osmosis (RO) is a type of membrane process which is considered as superior desalination technology, because of the less energy usage, lower costs and technological developments (Caldera et al., 2016; Pakdel et al., 2020).Therefore, , the RO membrane process has been considered as the desalination unit in this work. The amount of power consumed by SDS to remove salt from seawater and meet the potable water demand at time *t* and scenario *w* is expressed via equation (61), and water obtained from SDS is limited by equation (62) (Pakdel et al., 2020).

$$P_{t,w}^{D} = \eta^{D} Q_{t,w}^{D} \tag{61}$$

$$0 \le Q_{t,w}^{D} \le Q^{D,\max} \tag{62}$$

Total power consumption by water network consists of power consumed by SDS, water well pump and WST pump as equation (63).

$$P_{t,w}^{water} = P_{t,w}^{D} + P_{t,w}^{PWL} + P_{t,w}^{PS} \tag{63}$$

3.12. Multi-energy balance constraints:

According to equation (64), the electricity demand and power required by the water network, electric boiler, ISS charging, ESS charging and electricity sold to the main grid can be provided by the electricity purchased from the main network and power generated by the first and second type CHP units, wind turbine and ESS discharging. The gas imported from the main grid and GSS discharging, are provided the gas demand and gas needed for equipment such as first and second type CHP units, gas boiler and GSS charging, which is calculated by equation (65). The heat demand, the input heat of absorption chiller, HSS charging and heat sold to the main grid, must be met by purchasing heat from the main grid and heat generated by the first and second type CHP units, HSS discharging, electric boiler and gas boiler that is shown in equation (66). Equation (67) expresses that the cooling demand is supply by the absorption chiller and ISS discharging.

$$P_{t,w}^{EM,imp} - P_{t,w}^{EM,sell} + P_{t,w}^{wind} - P_{t,w}^{ch,ES} + P_{t,w}^{disch,ES} - EB_{t,w}^{eb} - P_{t,w}^{ch,ISS} - P_{t,w}^{Water} + \sum_{j=1}^{N_j} P_{t,w,j} = ED_{t,w}^{DR} \quad (64)$$

$$P_{t,w}^{GM,imp} - P_{t,w}^{ch,GS} + P_{t,w}^{disch,GS} - GB_{t,w}^{gb} - \sum_{j=1}^{N_j} GC_{t,w,j} = GD_t \quad (65)$$

$$P_{t,w}^{HM,imp} - P_{t,w}^{HM,sell} + H_{t,w}^{HS,\mathrm{dis}ch} - H_{t,w}^{HS,ch} + H_{t,w}^{gb} + H_{t,w}^{eb} - H_{t,w}^{abchlr} + \sum_{j=1}^{N_j} H_{t,w,j} = HD_t \quad (66)$$

$$C_{t,w}^{abchlr} + P_{t,w}^{disch,ISS} = CD_t \quad (67)$$

3.13. Multi-objective problem optimization:

3.13.1 The ε-constraint method:

In multi-objective problems, there is more than one objective, in which objective functions are entirely conflicting, and all objectives cannot be optimized simultaneously. Hence, decision-makers are looking to find the best solution. A technique for solving multi-objective problems is using the ε-constraint method, which is a practical solution for solving multi-objective problems with conflicting objective functions. Moreover, a multi-objective optimization problem such as equation (68) with *k* objectives could be solved using the ε-constraint method (Nazari-Heris et al., 2020).

$$\begin{aligned} &\max \quad (f_1(x), f_2(x), ..., f_k(x)) \\ &S.\ t. \\ &\qquad x \in R \end{aligned} \quad (68)$$

Where, x and R represent the decision variables and feasible region, respectively. According to this method, a multi-objective problem is solved by considering each objective function separately and converts to a single-objective problem. Thus, one of the objectives is considered as the main objective function so that this main objective function is optimized, while other objectives as constraints are considered, which is as follows:

$$\begin{aligned} &\max \quad f_1(x) \\ &S.t. \\ &\qquad f_2(x) \geq \varepsilon_2, \\ &\qquad f_3(x) \geq \varepsilon_3, \\ &\qquad \ldots \\ &\qquad f_k(x) \geq \varepsilon_k, \\ &\qquad x \in R \end{aligned} \tag{69}$$

In this study, the objective function associated with cost (including operation cost and emission cost) as the main objective function and objective function related to the amount of potable water extracted from the well as a constraint is considered. To obtain the optimal solution to the problem, the parameters of the ε-constraint method $(\varepsilon_2, \varepsilon_3, ..., \varepsilon_k)$ are changed parametrically. The values $(\varepsilon_2, \varepsilon_3, ..., \varepsilon_k)$ are based on the range of the k-1 objective functions.

3.13.2 Fuzzy approach:

By solving a multi-objective problem, the set of optimal solutions called the Pareto front is obtained, while only one optimal solution using the fuzzy approach can be selected, which is expressed as the best compromise solution. The fuzzy method assigns a fuzzy membership value in [0, 1] for each solution obtained in the Pareto front. The fuzzy membership function for the objective functions of this problem can be calculated as follows (Nazari-Heris et al., 2017):

$$f_k = \begin{cases} 1 & f_k < f_k^{\min} \\ \dfrac{f_k^{\max} - f_k}{f_k^{\max} - f_k^{\min}} & f_k^{\min} < f_k < f_k^{\max} \\ 0 & f_k > f_k^{\max} \end{cases} \tag{70}$$

The best compromise solution by using the min-max technique is obtained. According to this technique, the minimum value of f_1 and f_2 is provided, and then choosing the best compromise solution as the maximum amount of min (f_1, f_2). The flowchart of the whole problem optimization process is presented in Fig. 3.

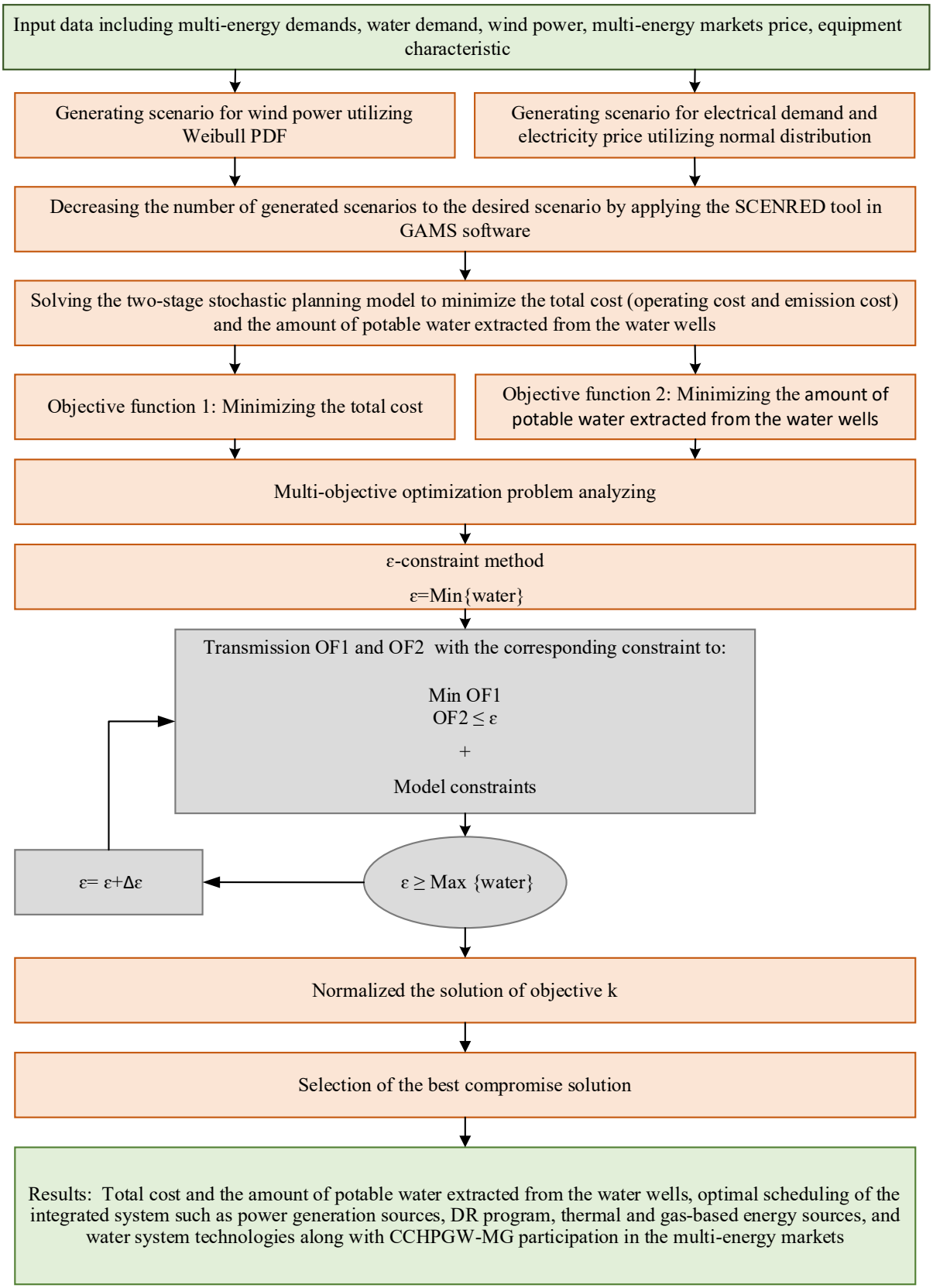

Fig. 3. Flowchart of the whole problem optimization process

4. Simulation and numerical results

4.1. Input data:

The proposed model is utilized for day-ahead scheduling of the CCHPGW-MG, as demonstrated in Fig. 1. Further the comprehensive information on CCHPGW-MG technologies and carbon emissions is presented in Table 2 (Agabalaye-Rahvar et al.; Mansour-Saatloo et al., 2020a; Mansour-Saatloo et al., 2020b; Pakdel et al., 2020). In addition, Table 3 is shown the FOR characteristics of the first and second type CHP units (Hadayeghparast et al., 2019). The microgrid operator is supplied via upstream electricity, gas and heating networks, wind turbines and water. The price prediction for the electricity, heat and gas market is illustrated in Fig. 4 (Mansour-Saatloo et al., 2020a; Murillo-Sánchez et al., 2013; Oskouei et al., 2021). Furthermore, Fig. 5 has observed the different demands, i.e., electricity, heat, cooling, gas and power generated through wind turbine (Mansour-Saatloo et al., 2020a; Mirzaei et al., 2021), while Fig. 6 presents the water demand (Pakdel et al., 2020).

To solve the mixed-integer non-linear programming (MINLP) problem, where the nonlinearity of the problem is due to the equations of the WST pump, the DICOPT solver in GAMS software is used. As mentioned above, a two-stage stochastic approach has introduced to manage the intermittent nature of electrical load, wind power and electricity price in the paper.

The Weibull PDF has included in numerous research papers for modeling wind power uncertainty because of its esteem adaptability (Mansour-Saatloo et al., 2020b). This study has deployed Weibull PDF to model wind power uncertainty, while the normal distribution has choosen to model electrical load and electricity price fluctuations.. In addition, the 1000 scenarios under mentioned uncertainties has been simulated by Monte Carlo method as it follows both Weibull PDF and normal distribution. . However, due to the computational complexity of the large number of scenarios, the generated scenarios have been reduced to 10 by the SCENRED tool in GAMS software. The SCENRED tool in GAMS software equipped with two scenario reduction approaches such as fast-backward approach and fast-forward approach. Specifically, the backward approach is faster compared to the forward approach in terms of computational time despite the accuracy, where the forward approach results are more accurate than the backward approach results with longer computational time.. SCENRED is capable of selecting

the desired number of preserved scenarios, named as Red_num_leaves. Further, the red_percentage operates according to the relative distance between the initial and decreased scenarios in SCENRED (Mirzaei et al., 2020b). In this study, a fast-backward scenario reduction algorithm has been applied with the Red_num_leaves factor of 10, to minimixe the computational complexity , the computational time and enhance the performance accuracy

Table 2. Data of the CCHPGW-MG technologies

	Parameter	Unit	Value		Parameter	Unit	Value
CHP units0	T_j^{ON}	h	2	**Ice storage**	$\eta^{ch,ISS}$	-	0.96
	T_j^{OFF}	h	2		$\eta^{disch,ISS}$	-	0.96
	η_{j1}	-	0.3		$E^{ISS,\max}$	kWh	200
	η_{j2}	-	0.35		$E^{ISS,\min}$	kWh	5
Gas boiler	η^{gb}	-	0.9		$P^{ch,ISS,\max}$	kW	50
	$H^{gb,\max}$	kW	80		$P^{ch,ISS,\min}$	kW	5
	$H^{gb,\min}$	kW	15		$P^{disch,ISS,\max}$	kW	50
Electrical boiler	η^{eb}	-	2		$P^{disch,ISS,\min}$	kW	5
	$H^{eb,\max}$	kW	40	**Absorption chiller**	η^{abchlr}	-	0.75
	$H^{eb,\min}$	kW	5		$C^{abchlr,\max}$	kW	70
Heat storage	η^{HS}	-	0.05		$C^{abchlr,\min}$	kW	10
	$\eta^{HS,ch}$	-	0.9	**Demand response**	DRE	%	10
	$\eta^{HS,disch}$	-	0.9		$C^{EL,up}$	\$/kWh	0.0025
	$E^{HS,\max}$	kWh	750		$C^{EL,dn}$	\$/kWh	0.0025
	$E^{HS,\min}$	kWh	0	**Carbon emission**	λ^C	\$/kg	0.02
	$E^{HS,\mathrm{ch},\max}$	kW	150		α	kg/kWh	0.92125
	$E^{HS,\mathrm{disch},\max}$	kW	150		β	kg/kWh	0.56267
Gas storage	$\eta^{ch,GS}$	-	0.95		γ	kg/kWh	0.2764
	$\eta^{disch,GS}$	-	0.95	**Water**	CS	m^2	4
	$E^{GS,\max}$	kWh	800		$LS^{\max}$	m	39.2
	$E^{GS,\min}$	kWh	0		$Q^{S,ch,\max}$	m^3/h	28
	$P^{ch,GS,\max}$	kW	200		$Q^{S,disch,\max}$	m^3/h	28
	$P^{ch,GS,\min}$	kW	20		L^{WL}	m	10
	$P^{disch,GS,\max}$	kW	200		g	m/s^2	9.81
	$P^{disch,GS,\min}$	kW	20		φ	kg/m^3	1000
Electrical storage	$\eta^{ch,ES}$	-	0.95		η^{PWL}	-	0.85
	$\eta^{disch,ES}$	-	0.95		η^{PS}	-	0.85
	$E^{ES,\max}$	kWh	600		η^{D}	kWh/m^3	3.0348
	$E^{ES,\min}$	kWh	60		L^G	m	4
	$P^{ch,ES,\max}$	kW	100		$Q^{D,\max}$	m^3/h	40
	$P^{ch,ES,\min}$	kW	20		LS_0	m	2
	$P^{disch,ES,\max}$	kW	100				

$P^{disch,ES,\min}$	kW	20	

Table 3. FOR characteristics of CHP units

The first type of CHP		**The second type of CHP**	
A (P, H)	(120, 0)	A (P, H)	(125.8, 0)
B (P, H)	(105, 87.5)	B (P, H)	(125.8, 32.4)
C (P, H)	(40, 50.9)	C (P, H)	(110.2, 135.6)
D (P, H)	(48, 0)	D (P, H)	(40, 75)
		E (P, H)	(44, 15.9)
		F (P, H)	(44, 0)

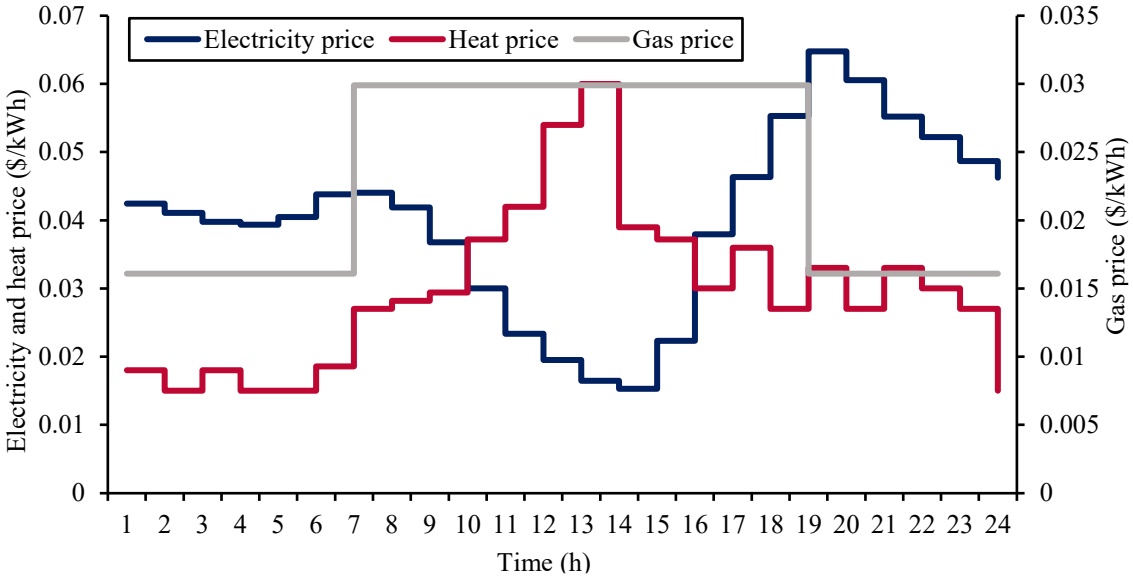

Fig. 4. Forecasted electricity, heat and gas market prices

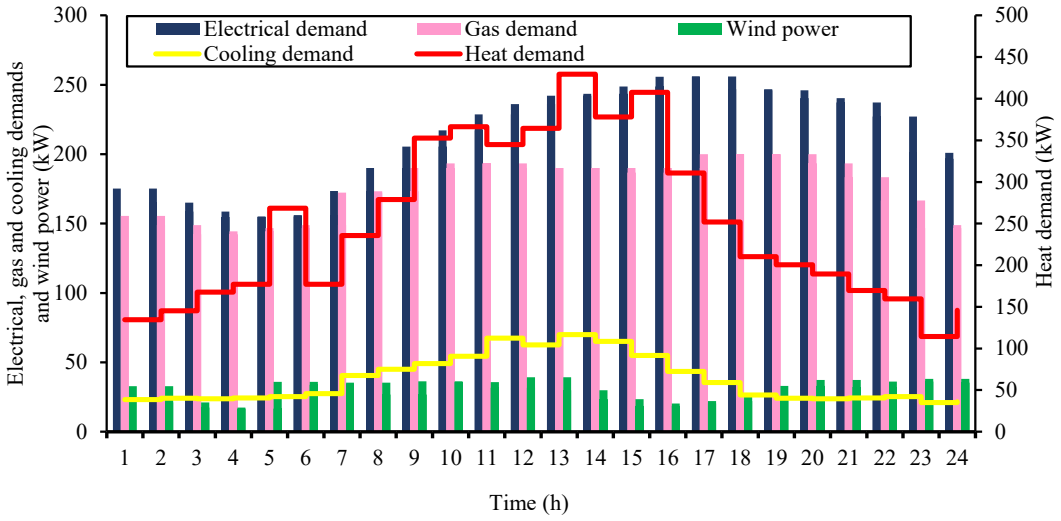

Fig. 5. Wind power and demands

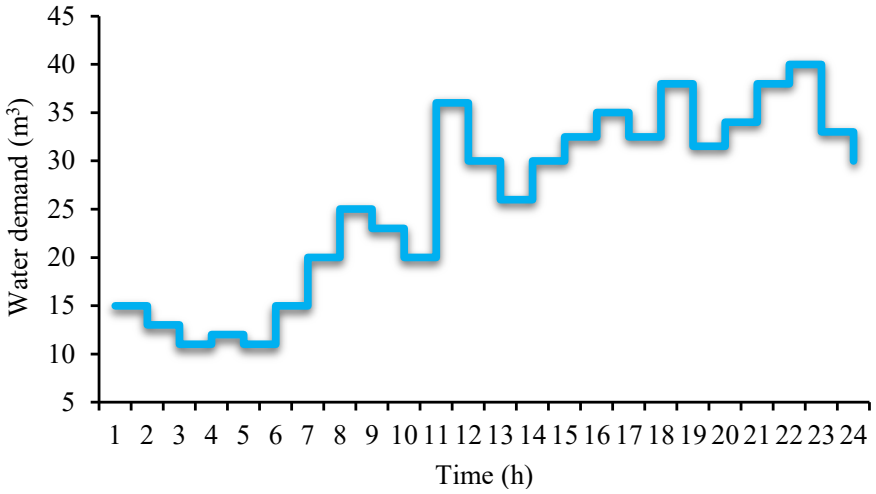

Fig. 6. Water demand

Table 4. The occurrence probability of scenarios

Scenario	W1	W2	W3	W4	W5	W6	W7	W8	W9	W10
Occurrence probability	0.115	0.232	0.044	0.061	0.065	0.015	0.141	0.185	0.116	0.026

4.2. Results:

In this work , an MINLP problem has been answered by DICOPT solver in GAMS software, where the number of single variables is chosen as 13474 and the number of single equations is selected as 19582. The optca and optcr options of the DICOPT solver to solve the MINLP problem are chosen as optca=0.0 and optcr=0.0. In fact, Optca option represents an absolute termination toleration for a solver of the global. When the absolute gap from optca option is not high , the solver stops. Optcr option specifies a relative termination toleration for a solver of the global. After evaluating an optimal solution which is between the range of specified toleration with optcr, the solver is stopped functioning while minimizing the solution time (Mirzaei et al., 2020a). Since the options optca=0.0 and optcr=0.0 , it is concluded that the optimality loss in this problem is zero. GAMS is an prominent optimization software to model mathematical problems and ideal for solving nonconvex and convex problems. Results gained from DICOPT solver could be provided a set of global optimality solutions to a reliable extent, which as been discussed in previous works (Ahrabi et al., 2021; Mirzaei et al., 2020a; Moazeni and Khazaei, 2020a, b; Moazeni et al., 2020; Pakdel et al., 2020). DICOPT solver is answered an MINLP problem

with the sub-problems of NLP and MIP, which NLP sub-problem solves through CONOPT solver and MIP sub-problem utilizes CPLEX solver. Moreover, Fig. 7 is illustrated the Flowchart of DICOPT solver to solve MINLP problem.

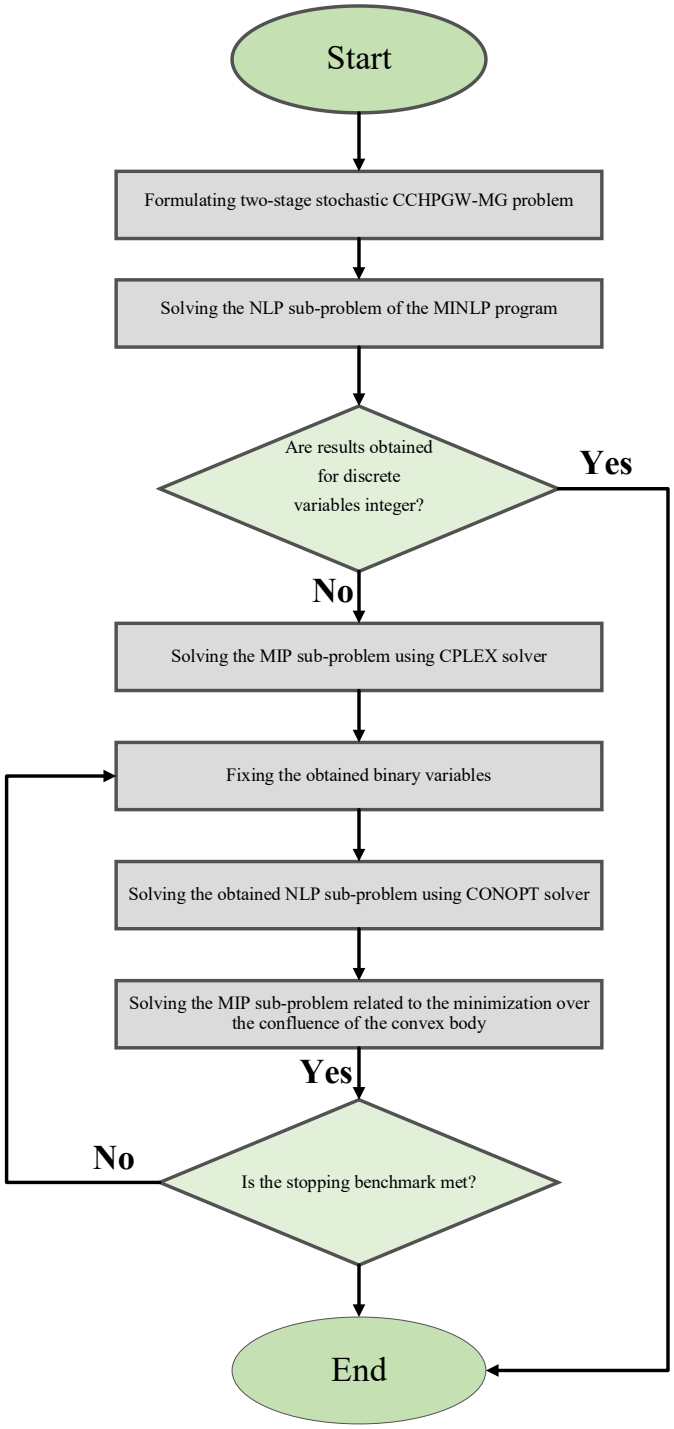

Fig. 7. Flowchart of DICOPT solver to solve MINLP program.

The optimal scheduling of water-energy sources of the proposed model is investigated under system uncertainties in three subsections.

4.2.1. The optimal scheduling of power-based sources and DR program along with CCHPGW-MG participation in the power market:

In this section, a multi-objective optimization problem is solved by considering uncertainties associated with electrical load, wind power and electricity price under a two-stage stochastic approach to minimize the total cost (operation cost and emission cost) and amount of potable water extracted from water wells, simultaneously. Fig. 8 shows the CCHPGW-MG Pareto optimal solutions using the ε-constraint method. Based on this figure, by increasing cost, the volume of water extracted from the well decreases. This means that from the point of view of the water objective function, to minimize the volume of water extracted from the well, the desalination unit must be used as much as possible to provide the water demand without extracting water from the well, which this subject increases the cost of operation, due to the desalination unit consumes the significant amount of energy. On the other hand, from the point of view of the cost objective function, the water demand must be met via water extracted from the well without using the desalination unit to minimize total cost. With respect to the value of fuzzy membership function in [0, 1], the production of Pareto optimal solutions with steps of 0.05 has proposed in this study, and the 21 iterations were selected to produce Pareto optimal solutions. As discussed before, the fuzzy approach is used to determine the best compromise solution. Based on Fig. 8, the optimal solution is achieved in the 16th iteration, where the value of the maximum weakest membership function in the 16th iteration equal to 0.750. According to the results of this iteration, the total cost and the amount of water extracted for the optimal solution equal to \$592.248 and 157.875 m^3, respectively.

Fig. 9 presents the electrical power supply and demand balance per hour. The expected optimal values of power above the horizontal axis/below the horizontal axis indicate the generation of electrical power/electrical power consumption. As seen in Fig. 9, the CCHPGW-MG operator buys power from the market as a consumer in hours when low electricity price (10 to 15) and sells power to the market

as a seller in hours when high electricity price (19 to 21), thus reducing costs. During off-peak electricity price hours, CHP units reduce their output power generation because purchase power from the market is more cost-effective than power generation via CHP units. However, at peak electricity price hours, these units increase their output power generation and provide part of the electrical demand. In addition, wind power meets part of the electrical demand at all hours. The ESS is operated at electricity price off-peak hours (10 to 15) in the charging mode, then at electricity price peak hours (18 to 22) is operated in the discharging mode. The water network consumes power at all hours to meet the required water demand, but as depicted in Fig. 9, the amount of power consumed via the water network during off-peak hours of electricity price is higher than peak hours of electricity price. The ISS also consumes power, during off-peak hours of electricity price to supply cooling demand, in other words, in this state the ISS is operated in charging mode. Furthermore, due to the dependence of the electric boiler on the market price of electricity and heat, it is more economical (for example, between t=6 and t=19) to participate in the power market. The impact of the ESS and DR program on the power exchange with the market is shown in Fig. 10. As obvious in this figure, due to the presence of ESS and DR, the amount of power sold to market during peak hours of electricity price (19 to 21) and the purchased power from the market during off-peak hours of electricity price (10 to 15) significantly has increased. Also, the effect of ESS is much rather than the DR program. Fig. 11 represents the variation of electrical demand by applying the DR program. According to this figure, the electrical demand has been shifted from electricity price peak hours (18 to 23) to electricity price off-peak hours (10 to 15).

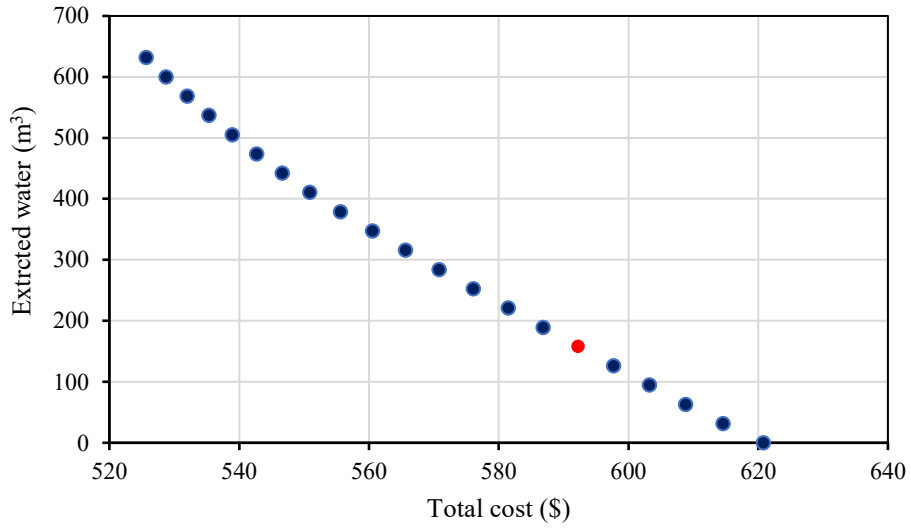

Fig. 8. Pareto optimal solutions to the multi-objective problem

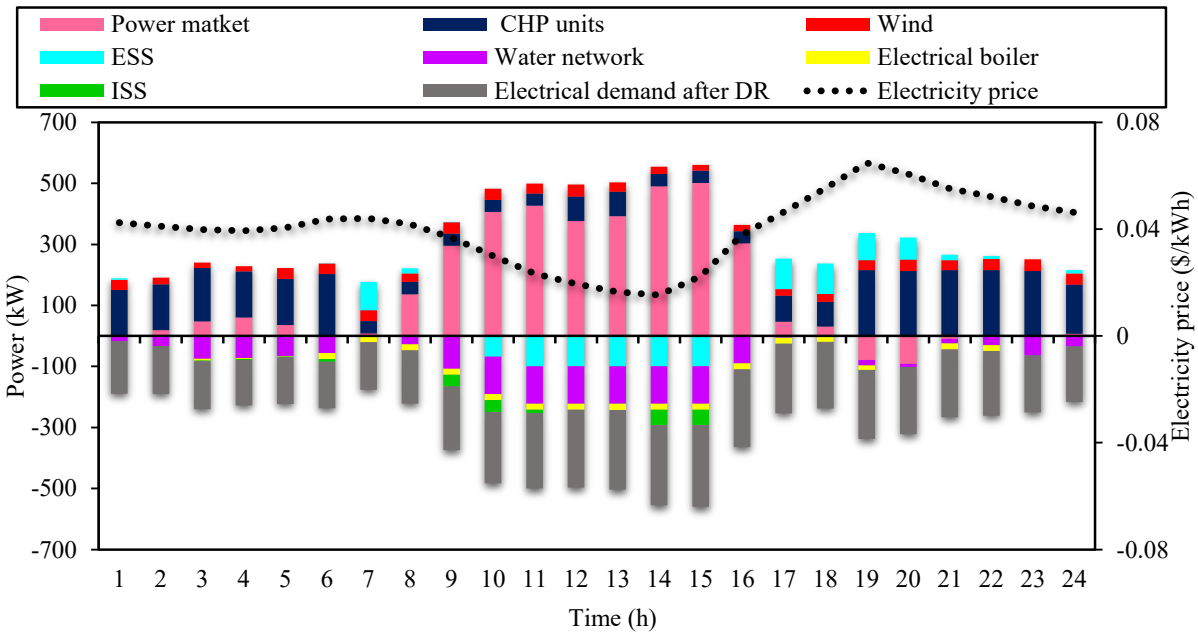

Fig. 9. Electrical power supply and demand balance in the CCHPGW-MG

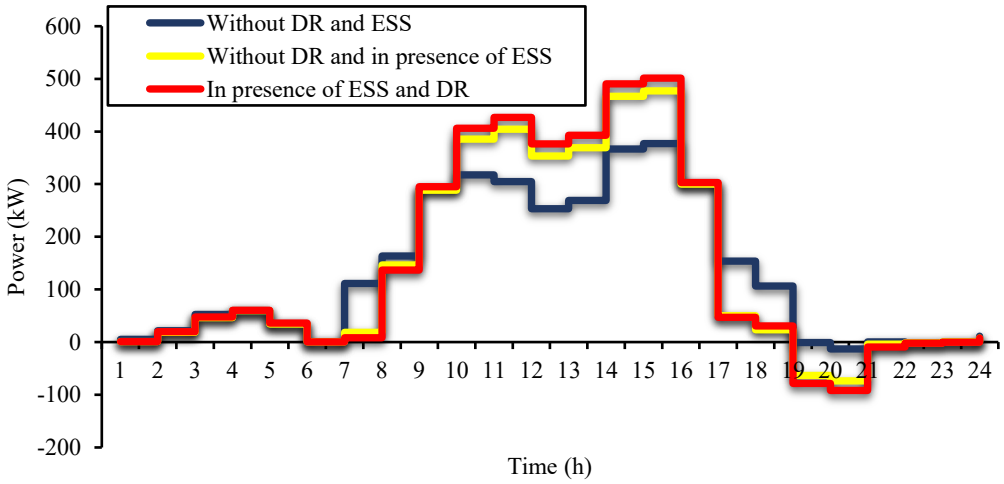

Fig. 10. The impact of ESS and DR program on the power exchange with the market

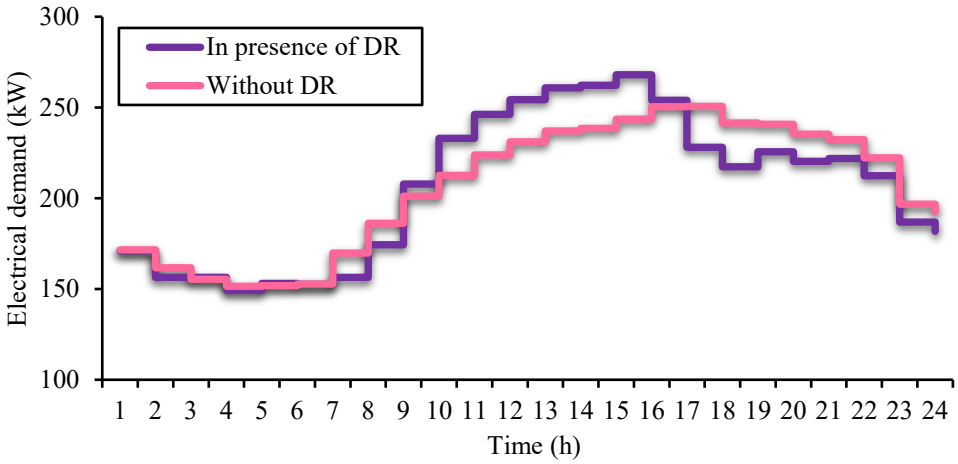

Fig. 11. The variation of electrical demand applying the DR program

4.2.2. The optimal scheduling of thermal and gas-based energy sources along with CCHPGW-MG participation in the heat, gas and power market:

In this section, based on the optimal solution obtained from solving the multi-objective optimization problem in the previous section, the optimal scheduling of the thermal and gas-based energy sources is investigated. The heating power supply and demand balance demonstrate in Fig. 12. The expected optimal values of heat above and below the horizontal axis illustrate the generation and consumption of the heat, respectively. It can be obvious in this figure that a significant part of the heat demand is met via CHP units. As mentioned earlier, due to the electrical boiler's dependence on the market price of electricity and heat, it is more economical for this unit (for example, between t=6 and t=19) to generate heat.

The gas boiler is also applied in most hours to supply the heat demand at its maximum capacity. The HSS dependent on the heat market price and heat generation by the CHP units, so in hours when the market price of heat is low and the amount of heat generated via CHP units is high (t=1-6 and t=23-24) is operated in the charge mode, and then during the hours when the market price of heat is high and the amount of heat generated via CHP units is low (10 to 13) is operated in the discharge mode. Furthermore, the CCHPGW-MG operator buys heat from the market as a consumer in hours when the amount of heat generated by the CHP units is low (t=7-11 and t=13-18) and then sell the heat to the market as a seller in hours when the amount of heat generated by the CHP units is high (19 to 23). The absorption chiller also uses heat at all hours to provide the cooling demand. Fig. 13 shows the gas supply and demand balance. The expected optimal values of gas above and below the horizontal axis demonstrate the generation and consumption of the gas, respectively. According to this figure, CHP units consumes gas at all hours to meet power and heat demand, so that the amount of gas consumed via CHP units during gas price peak hours (7 to 18) is much less the amount of gas consumed during gas price off-peak hours (t=1-6 and t=19-24). Also, the CCHPGW-MG operator prefers to buy less gas from the market during peak gas price hours. Due to the dependence of GSS on the price of the gas market is operated in the charging mode at gas price off-peak hours (t=2,4,5,6 and t=22-24) and then is

operated in the discharging mode at gas price peak hours (7 to 11). In addition, due to the low price of the gas market, the gas boiler also consumes gas in most hours to supply the heat demand.

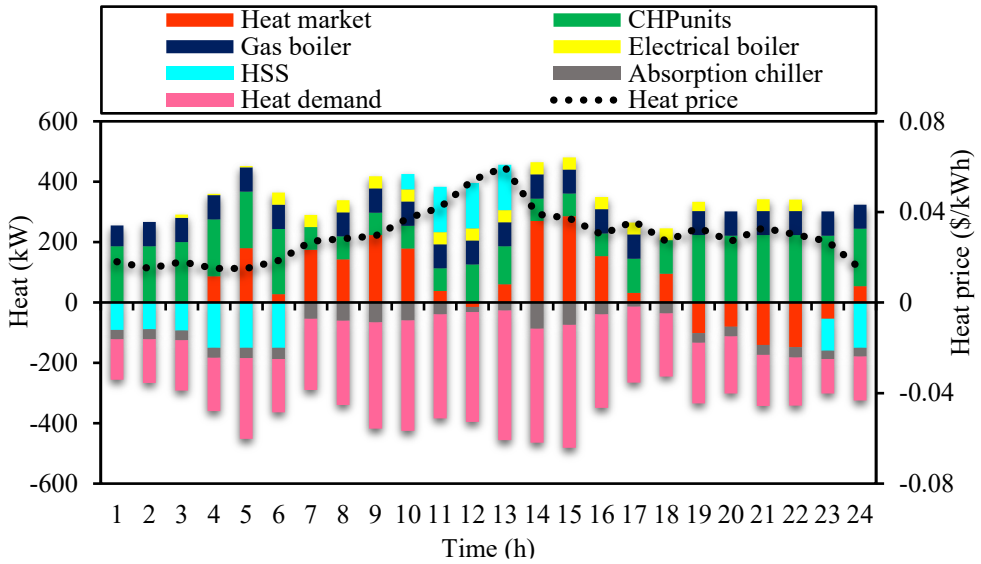

Fig. 12. Heating power supply and demand balance in the CCHPGW-MG

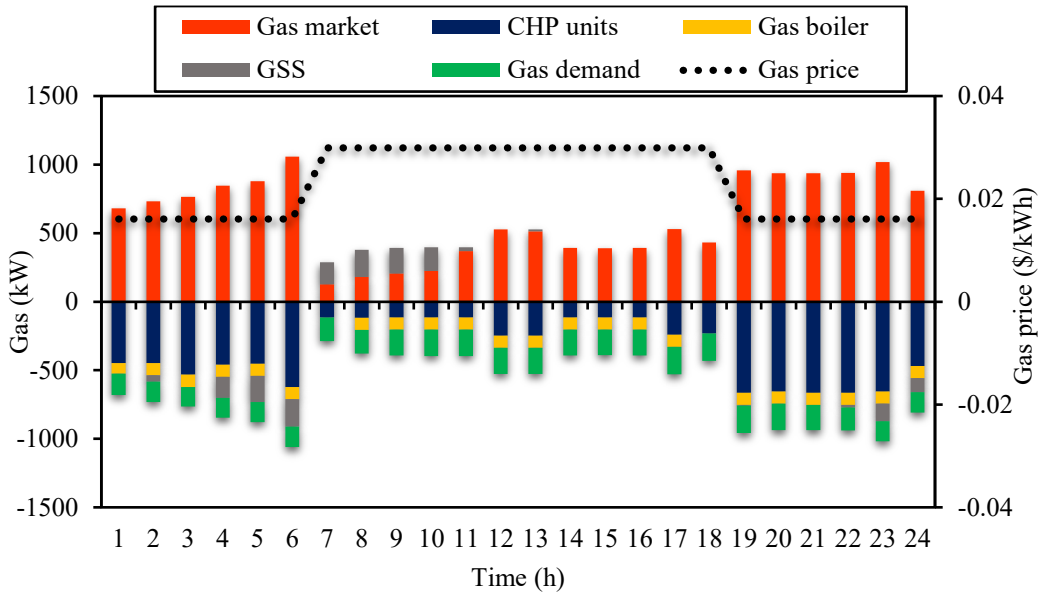

Fig. 13. Gas supply and demand balance in the CCHPGW-MG

Fig. 14 presents the cooling power supply and demand balance. The expected optimal values of cooling power above and below the horizontal axis indicate the generation and consumption of the cooling power, respectively. As can be seen in Fig. 14, the cooling demand is met by the chiller and the ISS, so that the chiller is applied at all hours to provide the cooling demand, but in the hours when the cooling demand and the heat market price are high (for example, t=11-13), it is more economical where part of

the cooling demand to be met by the ISS, in other words, in this state the ISS is operated in discharging mode. In Fig. 15, the impact of HSS on the heat market is presented. Based on this figure, due to the presence of HSS, in off-peak hours of heat price (4 to 6), the more heat is purchased from the heat market, and then in peak hours of heat price (10 to 13), the less heat is purchased from the heat market. In Fig. 16, the impact of GSS on the gas market is illustrated. As depicted in this figure, similar to the HSS analysis, the amount of gas purchased from the gas market increases during the hours when the gas price is low (4 to 6), and then the amount of gas purchased from the gas market decreases during the hours when the gas price is high (7 to 11). In Fig. 17, the impact of ISS on the heat and power market is demonstrated. As mentioned earlier, the ISS meets part of the cooling demand by consuming power, therefore its effects on both the heat and power market. Based on this figure, due to the presence of ISS, the amount of heat purchased from the heat market during heat price peak hours (10 to 13) has decreased, moreover the ISS is purchased its required power during off-peak hours of electricity price (t=9,10,11,14,15) from the power market.

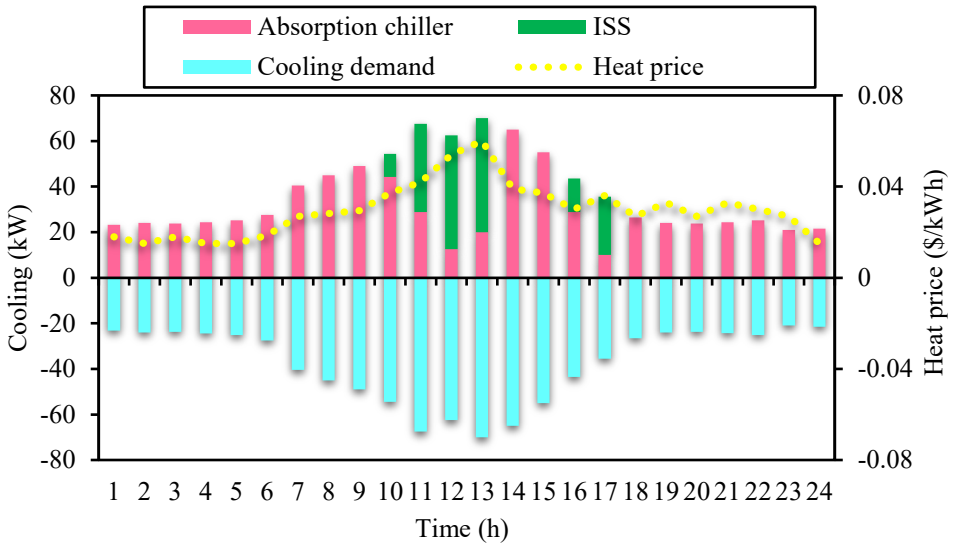

Fig. 14. Cooling power supply and demand balance in the CCHPGW-MG

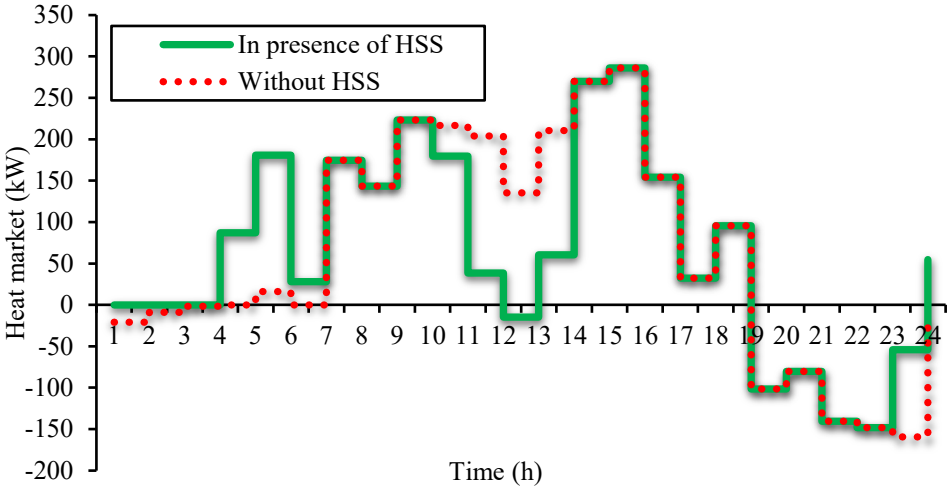

Fig. 15. The impact of HSS on the heat market

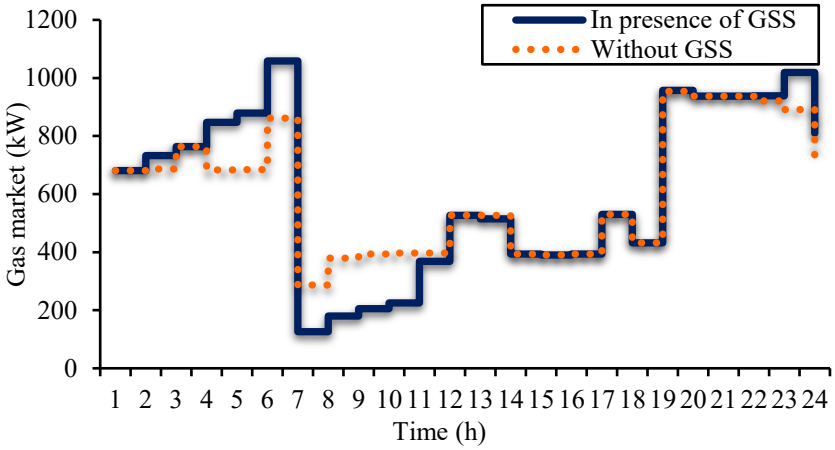

Fig. 16. The impact of GSS on the gas market

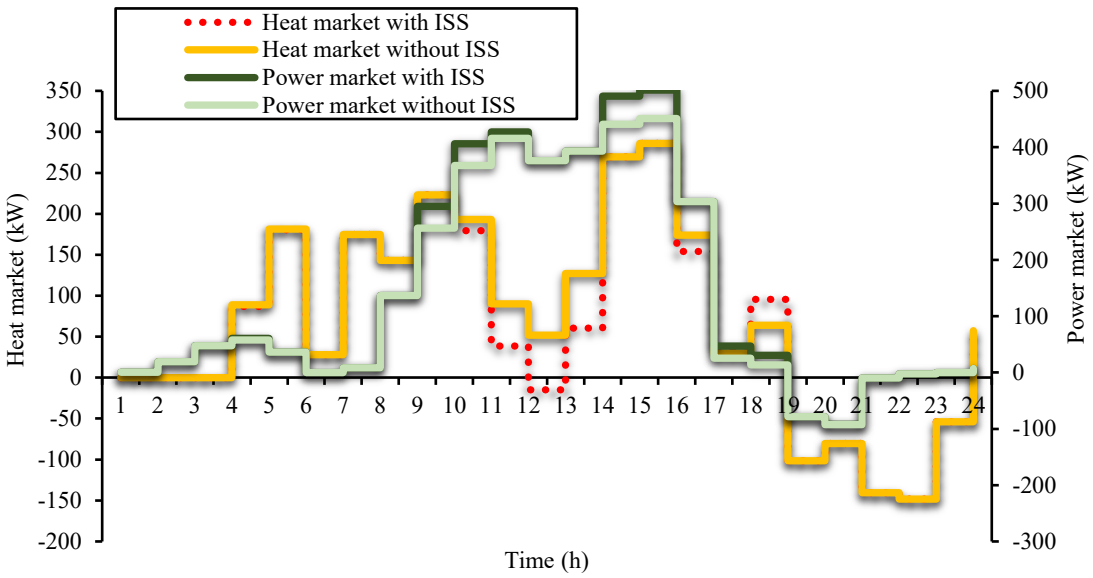

Fig. 17. The impact of ISS on the heat and power market

4.2.3. The optimal scheduling of water system technologies along with CCHPGW-MG participation in the power market:

In this section, according to the optimal solution achieved from solving the multi-objective optimization problem in the first section, the optimal scheduling of water system technologies is investigated. Fig. 18 presents the water network supply and demand balance, per hour. The expected optimal values of water system technologies above and below the horizontal axis illustrate the generation and consumption of the water network, respectively. From the environmental aspect, the SDS has a significant effect on the optimization problem. However, as mentioned earlier, this unit consumes a considerable amount of power, therefore as shown in Fig. 18, the SDS is applied only at electricity price off-peak hours (10 to 15) at its maximum capacity, and at other hours, it is much less applied. In addition, the WST pump consumes power when it is in the charging mode, hence the WST is operated during off-peak hours of the electricity price (9 to 16) in the charging mode, and then during peak hours of the electricity price (17 to 23) in the discharging mode is operated, and accordingly provides part of the water demand. Furthermore, during peak hours of the electricity price that the use of SDS is not economical; it is more cost-effective to meet water demand via water extracted from the water wells and the WST. Fig. 19 represents the impact of WST on the power market. As can be obvious in this figure, the WST has purchased the power required for its performance during electricity price off-peak hours (for example, 9 to 15) from the power market. Table 5 demonstrates the impact of multi-energy storage systems, WST and DR program on the total cost (operating cost and emission cost). As can be seen from the obtained simulation results, the calculation of the total cost excludes multi-energy storage systems, WST and DR program is \$632.653, while in the presence of multi-energy storage systems, WST and DR program the total cost is reduced to \$592.248, which represents a 6.82% reduction in the total costs of the CCHPGW-MG. Therefore, it can be resulted that the use of multi-energy storage systems, WST and DR program has a significant effect on reducing operating cost and emission cost. Also, according to results obtained from the simulation, WST has decreased the volume of freshwater extracted from water wells from 181.863 m^3 to 157.875 m^3. In addition, with the performed analysis on increasing of adjustable electrical load value up to 20%, the total cost has reduced to \$589.640.

In addition, , the computational time for the entire system could be calculates as 21.615 (Second), and the computational time for each part is given in Table 5. The multi-energy microgrids are extremely popular among researches at present and some researches have considered various ranges for microgrids as kW (e.g., 160 kW-700 kW) and as MW (e.g., by 45 MW) (Is there any specific power rating what kW or MW for microgrid, n.d.). Therefore, it is clear that the renewable energy microgrids with photovoltaic system, wind turbine, electrical storage systems and power convertor could be utilized in the large-scale microgrids. For example, (He et al., 2018). These results are concluded that the large scale microgrid could be implemented by the proposed work.

Table 5. The impact of multi-energy storage systems, WST and DR program on the total cost and the computational time

Storages and DR	**-**	**ESS**	**GSS**	**HSS**	**ISS**	**WST**	**DR**	**Multi-energy storages and DR**
Total cost ($) (Operating cost and emission cost)	632.653	620.790	623.941	625.962	626.757	626.778	629.088	592.248
computational time (Second)	03:012	04.563	03.941	03.570	05.345	06.697	03.924	21.615

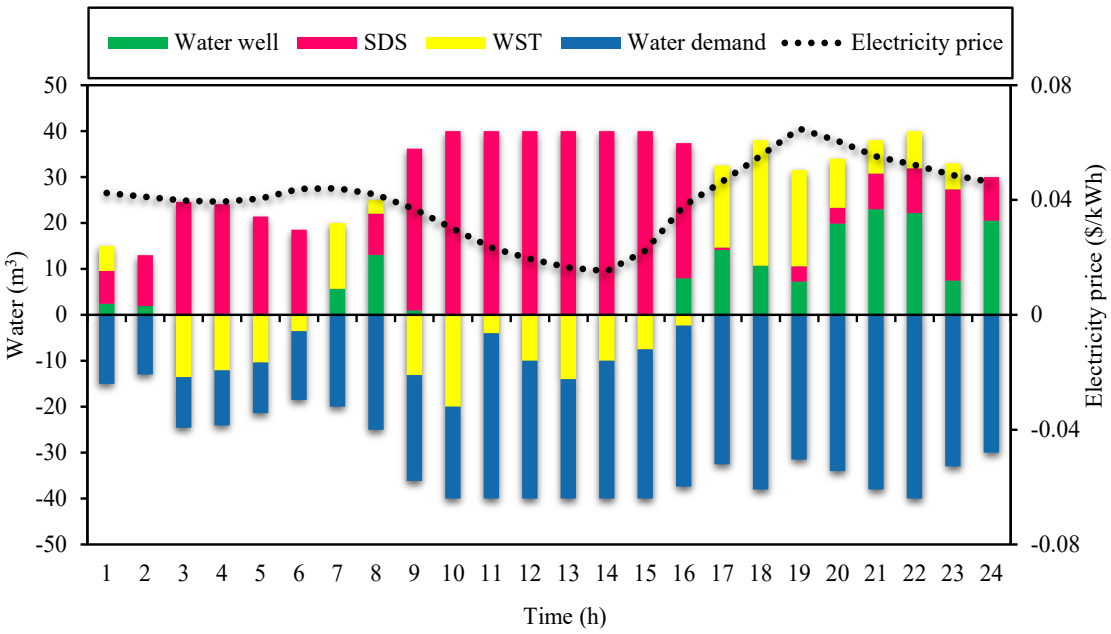

Fig. 18. Water network supply and demand balance in the CCHPGW-MG

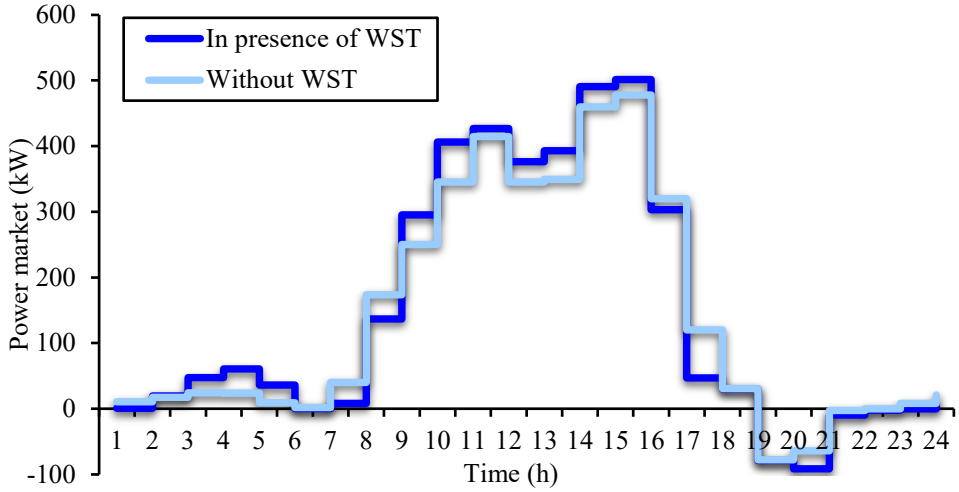

Fig. 19. The impact of WST on the power market

5. Conclusion

This paper proposed an optimal scheduling model for a developed microgrid called combined cooling, heating, power, gas and water-based microgrid (CCHPGW-MG). A multi-objective optimization problem was introduced to minimize the operating cost, emission cost, and freshwater volume extracted from water wells, which was solved utilizing the epsilon constraint method. The major problem of designing the multi-objective problem was the antonym behavior to reduce the energy cost besides water generation via seawater desalination system (SDS) . This study has evaluated under two prime factors which the first aspect was related to environmental and economic problems, and the second aspect was fascinated by the underground reservoirs of the potable water and water crisis. Furthermore, a two-stage stochastic approach was applied to manage the uncertainties associated with electrical load, wind power and electricity price in the CCHPGW-MG. The use of seawater desalination system (SDS) technology not only cause to reduce environmental pollution but also decrease the extraction of potable water from underground reservoirs. Since the SDS consumes a significant amount of power for its performance, the water storage tank (WST) was applied to meet part of the water demand during electricity price peak hours to reduce total cost. The role of multi-energy storage systems such as heat storage system (HSS), electrical storage system (ESS), gas storage system (GSS), ice storage system (ISS) and water storage tank (WST), as well as the DR program, have been evaluated on the operation of the integrated system. By simultaneously considering water system technologies such as SDS, WST,

and water well, not only has been decreased the volume of freshwater extracted from water wells, but also from economic and environmental aspects is affected the optimal operating of the proposed model. In particular, , the optimal operation of the water sector technologies would enhance the energy systems optimal operation to benefit the entire system.,. The numerical results illustrated the following points:

1) Multi-energy storage systems, WST along with DR program, have been reduced the total cost, including operating cost and emission cost, by 6.82%.
2) WST has been decreased the value of potable water extracted from water wells by 15.2%.
3) The integrated scheduling model of the energy-water system, in addition to the total cost reduction, has been reduced the volume of freshwater extracted from underground reservoirs by 64%.

References:

Agabalaye-Rahvar, M., Mansour-Saatloo, A., Mirzaei, M.A., Mohammadi-Ivatloo, B., Zare, K., Economic-environmental stochastic scheduling for hydrogen storage-based smart energy hub coordinated with integrated demand response program. International Journal of Energy Research.

Ahmadi, E., McLellan, B., Ogata, S., Mohammadi-Ivatloo, B., Tezuka, T., 2020. An Integrated Planning Framework for Sustainable Water and Energy Supply. Sustainability 12(10), 4295.

Ahrabi, M., Abedi, M., Nafisi, H., Mirzaei, M.A., Mohammadi-Ivatloo, B., Marzband, M., 2021. Evaluating the effect of electric vehicle parking lots in transmission-constrained AC unit commitment under a hybrid IGDT-stochastic approach. International Journal of Electrical Power & Energy Systems 125, 106546.

Amir, V., Azimian, M., 2020. Dynamic Multi-Carrier Microgrid Deployment Under Uncertainty. Applied Energy 260, 114293.

Caldera, U., Bogdanov, D., Breyer, C., 2016. Local cost of seawater RO desalination based on solar PV and wind energy: A global estimate. Desalination 385, 207-216.

Cui, Q., Ma, P., Huang, L., Shu, J., Luv, J., Lu, L., 2020. Effect of device models on the multiobjective optimal operation of CCHP microgrids considering shiftable loads. Applied Energy 275, 115369.

Dai, J., Wu, S., Han, G., Weinberg, J., Xie, X., Wu, X., Song, X., Jia, B., Xue, W., Yang, Q., 2018. Water-energy nexus: A review of methods and tools for macro-assessment. Applied Energy 210, 393-408.
Daneshvar, M., Mohammadi-Ivatloo, B., Asadi, S., Anvari-Moghaddam, A., Rasouli, M., Abapour, M., B. Gharehpetian, G., 2020. Chance-constrained models for transactive energy management of interconnected microgrid clusters. Journal of Cleaner Production 271.
Ding, X., Guo, Q., Qiannan, T., Jermsittiparsert, K., 2021. Economic and environmental assessment of multi-energy microgrids under a hybrid optimization technique. Sustainable Cities and Society 65, 102630.
Ehsan, A., Yang, Q., 2019. Scenario-based investment planning of isolated multi-energy microgrids considering electricity, heating and cooling demand. Applied Energy 235, 1277-1288.
Fateh, H., Bahramara, S., Safari, A., 2020. Modeling operation problem of active distribution networks with retailers and microgrids: A multi-objective bi-level approach. Applied Soft Computing 94, 106484.
Feizizadeh, B., Ronagh, Z., Pourmoradian, S., Gheshlaghi, H.A., Lakes, T., Blaschke, T., 2021. An efficient GIS-based approach for sustainability assessment of urban drinking water consumption patterns: A study in Tabriz city, Iran. Sustainable Cities and Society 64, 102584.
Hadayeghparast, S., Farsangi, A.S., Shayanfar, H., 2019. Day-ahead stochastic multi-objective economic/emission operational scheduling of a large scale virtual power plant. Energy 172, 630-646.
He, L., Zhang, S., Chen, Y., Ren, L., Li, J., 2018. Techno-economic potential of a renewable energy-based microgrid system for a sustainable large-scale residential community in Beijing, China. Renewable and Sustainable Energy Reviews 93, 631-641.
Hemmati, M., Mohammadi-Ivatloo, B., Abapour, M., Anvari-Moghaddam, A., 2020. Optimal Chance-Constrained Scheduling of Reconfigurable Microgrids Considering Islanding Operation Constraints. IEEE Systems Journal.
Hemmati, M., Mohammadi-Ivatloo, B., Ghasemzadeh, S., Reihani, E., 2018. Risk-based optimal scheduling of reconfigurable smart renewable energy based microgrids. International Journal of Electrical Power & Energy Systems 101, 415-428.
Hou, H., Xue, M., Xu, Y., Xiao, Z., Deng, X., Xu, T., Liu, P., Cui, R., 2020. Multi-objective economic dispatch of a microgrid considering electric vehicle and transferable load. Applied Energy 262, 114489.
Is there any specific power rating what kW or MW for microgrid, n.d. Retrieved from https://www.researchgate.net/post/Is_there_any_specific_power_rating_what_kW_or_MW_for_Microgrid.
Jahani, A., Zare, K., Khanli, L.M., Karimipour, H., 2021. Optimized Power Trading of Reconfigurable Microgrids in Distribution Energy Market. IEEE Access 9, 48218-48235.
Li, M., Fu, Q., Singh, V.P., Ji, Y., Liu, D., Zhang, C., Li, T., 2019. An optimal modelling approach for managing agricultural water-energy-food nexus under uncertainty. Science of the Total Environment 651, 1416-1434.
Li, Q., Yu, S., Al-Sumaiti, A.S., Turitsyn, K., 2018. Micro water–energy nexus: Optimal demand-side management and quasi-convex hull relaxation. IEEE Transactions on Control of Network Systems 6(4), 1313-1322.
Li, Z., Xu, Y., 2019. Temporally-coordinated optimal operation of a multi-energy microgrid under diverse uncertainties. Applied Energy 240, 719-729.
Mansour-Saatloo, A., Agabalaye-Rahvar, M., Mirzaei, M.A., Mohammadi-Ivatloo, B., Abapour, M., Zare, K., 2020a. Robust scheduling of hydrogen based smart micro energy hub with integrated demand response. Journal of Cleaner Production 267, 122041.
Mansour-Saatloo, A., Mirzaei, M.A., Mohammadi-Ivatloo, B., Zare, K., 2020b. A risk-averse hybrid approach for optimal participation of power-to-hydrogen technology-based multi-energy microgrid in multi-energy markets. Sustainable Cities and Society 63, 102421.

Mirzaei, M.A., Hemmati, M., Zare, K., Abapour, M., Mohammadi-Ivatloo, B., Marzband, M., Anvari-Moghaddam, A., 2020a. A novel hybrid two-stage framework for flexible bidding strategy of reconfigurable micro-grid in day-ahead and real-time markets. International Journal of Electrical Power & Energy Systems 123, 106293.
Mirzaei, M.A., Nazari-Heris, M., Mohammadi-Ivatloo, B., Zare, K., Marzband, M., Anvari-Moghaddam, A., 2020b. Hourly Price-Based Demand Response for Optimal Scheduling of Integrated Gas and Power Networks Considering Compressed Air Energy Storage, Demand Response Application in Smart Grids. Springer, pp. 55-74.
Mirzaei, M.A., Oskouei, M.Z., Mohammadi-Ivatloo, B., Loni, A., Zare, K., Marzband, M., Shafiee, M., 2020c. Integrated energy hub system based on power-to-gas and compressed air energy storage technologies in the presence of multiple shiftable loads. IET Generation, Transmission & Distribution 14(13), 2510-2519.
Mirzaei, M.A., Zare, K., Mohammadi-Ivatloo, B., Marzband, M., Anvari-Moghaddam, A., 2021. Robust network-constrained energy management of a multiple energy distribution company in the presence of multi-energy conversion and storage technologies. Sustainable Cities and Society 74, 103147.
Moazeni, F., Khazaei, J., 2020a. Dynamic economic dispatch of islanded water-energy microgrids with smart building thermal energy management system. Applied Energy 276, 115422.
Moazeni, F., Khazaei, J., 2020b. Optimal operation of water-energy microgrids; a mixed integer linear programming formulation. Journal of Cleaner Production 275, 122776.
Moazeni, F., Khazaei, J., 2021. Optimal energy management of water-energy networks via optimal placement of pumps-as-turbines and demand response through water storage tanks. Applied Energy 283, 116335.
Moazeni, F., Khazaei, J., Mendes, J.P.P., 2020. Maximizing energy efficiency of islanded micro water-energy nexus using co-optimization of water demand and energy consumption. Applied Energy 266, 114863.
Murillo-Sánchez, C.E., Zimmerman, R.D., Anderson, C.L., Thomas, R.J., 2013. Secure planning and operations of systems with stochastic sources, energy storage, and active demand. IEEE Transactions on Smart Grid 4(4), 2220-2229.
Murty, V., Kumar, A., 2020. Multi-objective energy management in microgrids with hybrid energy sources and battery energy storage systems. Protection and Control of Modern Power Systems 5(1), 1-20.
Najafi, J., Peiravi, A., Anvari-Moghaddam, A., Guerrero, J.M., 2019. Resilience improvement planning of power-water distribution systems with multiple microgrids against hurricanes using clean strategies. Journal of cleaner production 223, 109-126.
Nami, H., Anvari-Moghaddam, A., Arabkoohsar, A., 2020. Application of CCHPs in a centralized domestic heating, cooling and power network—Thermodynamic and economic implications. Sustainable Cities and Society 60, 102151.
Nazari-Heris, M., Abapour, S., Mohammadi-Ivatloo, B., 2017. Optimal economic dispatch of FC-CHP based heat and power micro-grids. Applied Thermal Engineering 114, 756-769.
Nazari-Heris, M., Mirzaei, M.A., Mohammadi-Ivatloo, B., Marzband, M., Asadi, S., 2020. Economic-environmental effect of power to gas technology in coupled electricity and gas systems with price-responsive shiftable loads. Journal of Cleaner Production 244, 118769.
Oskouei, M.Z., Mirzaei, M.A., Mohammadi-Ivatloo, B., Shafiee, M., Marzband, M., Anvari-Moghaddam, A., 2021. A hybrid robust-stochastic approach to evaluate the profit of a multi-energy retailer in tri-layer energy markets. Energy 214, 118948.

Pakdel, M.J.V., Sohrabi, F., Mohammadi-Ivatloo, B., 2020. Multi-objective optimization of energy and water management in networked hubs considering transactive energy. Journal of Cleaner Production, 121936.
Pourghasem, P., Sohrabi, F., Abapour, M., Mohammadi-Ivatloo, B., 2019. Stochastic multi-objective dynamic dispatch of renewable and CHP-based islanded microgrids. Electric Power Systems Research 173, 193-201.
Roustaei, M., Niknam, T., Salari, S., Chabok, H., Sheikh, M., Kavousi-Fard, A., Aghaei, J., 2020. A scenario-based approach for the design of Smart Energy and Water Hub. Energy 195.
Saberi, K., Pashaei-Didani, H., Nourollahi, R., Zare, K., Nojavan, S., 2019. Optimal performance of CCHP based microgrid considering environmental issue in the presence of real time demand response. Sustainable cities and society 45, 596-606.
Shang, Y., Hei, P., Lu, S., Shang, L., Li, X., Wei, Y., Jia, D., Jiang, D., Ye, Y., Gong, J., 2018. China's energy-water nexus: Assessing water conservation synergies of the total coal consumption cap strategy until 2050. Applied Energy 210, 643-660.
Sui, Q., Wei, F., Lin, X., Li, Z., 2021. Optimal energy management of a renewable microgrid integrating water supply systems. International Journal of Electrical Power & Energy Systems 125, 106445.
Wang, X.-C., Jiang, P., Yang, L., Van Fan, Y., Klemeš, J.J., Wang, Y., 2021. Extended water-energy nexus contribution to environmentally-related sustainable development goals. Renewable and Sustainable Energy Reviews 150, 111485.
Wang, X.-C., Klemeš, J.J., Wang, Y., Dong, X., Wei, H., Xu, Z., Varbanov, P.S., 2020. Water-Energy-Carbon Emissions nexus analysis of China: An environmental input-output model-based approach. Applied Energy 261, 114431.
Wang, Y., Tang, L., Yang, Y., Sun, W., Zhao, H., 2020. A stochastic-robust coordinated optimization model for CCHP micro-grid considering multi-energy operation and power trading with electricity markets under uncertainties. Energy, 117273.
Wei, J., Zhang, Y., Wang, J., Cao, X., Khan, M.A., 2020a. Multi-period planning of multi-energy microgrid with multi-type uncertainties using chance constrained information gap decision method. Applied Energy 260, 114188.
Wei, J., Zhang, Y., Wang, J., Cao, X., Khan, M.A., 2020b. Multi-period planning of multi-energy microgrid with multi-type uncertainties using chance constrained information gap decision method. Applied Energy 260.
Wu, Y., Wang, X., Fu, Y., Xu, Y., 2017. Difference brain storm optimization for combined heat and power economic dispatch, International Conference on Swarm Intelligence. Springer, pp. 519-527.
Yang, Y., Tang, L., Wang, Y., Sun, W., 2020. Integrated operation optimization for CCHP micro-grid connected with power-to-gas facility considering risk management and cost allocation. International Journal of Electrical Power & Energy Systems 123, 106319.
Zhang, W., Valencia, A., Gu, L., Zheng, Q.P., Chang, N.-B., 2020. Integrating emerging and existing renewable energy technologies into a community-scale microgrid in an energy-water nexus for resilience improvement. Applied Energy 279, 115716.
Zhou, Y., Shahidehpour, M., Wei, Z., Li, Z., Sun, G., Chen, S., 2019. Distributionally robust unit commitment in coordinated electricity and district heating networks. IEEE Transactions on Power Systems 35(3), 2155-2166.